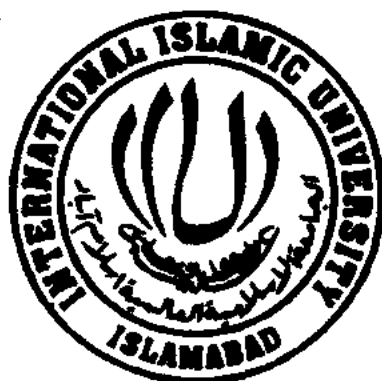


**Study of Fe Doped Induced Effects on Physical Properties
of CuO Nanostructures**



MS Thesis

By

Asghar Ali

Supervised by

Dr. Javed Iqbal Saggu

Department of Physics

Faculty of Basic and Applied Sciences

International Islamic University Islamabad

(2015)



TH-14516

④ 93

MS
2005

C2

10/10/05

10/10/05

10/10/05

Certificate

This is to certify that the work contained in this thesis entitled: “**Study of Fe Doped Induced Effects on Physical Properties of CuO Nanostructures**” has been carried out by **Asghar Ali** in Laboratory of Nanoscience and Technology (LNT) under my supervision. In my opinion, this is fully adequate in scope and quality for the degree of MS Physics.



Supervisor

Department of Physics

International Islamic University

Dr. Javed Iqbal Saggu
Assistant Professor (Physics)
International Islamic University
Islamabad.

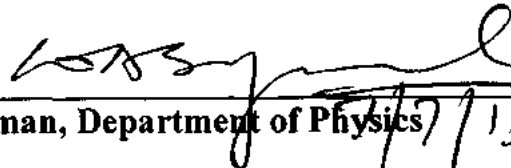
Study of Fe Doped Induced Effects on Physical Properties of CuO Nanostructures

By

Asghar Ali

(152-FBAS/MSPHY/S13)

This Thesis submitted to Department of Physics
International Islamic University, Islamabad
for the award of degree of MS Physics



Chairman, Department of Physics

International Islamic University Islamabad

**CHAIRMAN
DEPT. OF PHYSICS
International Islamic University
Islamabad**



**Dean, Faculty of Basic and Applied Science
International Islamic University, Islamabad**

Final Approval

This is to certify that the work contained in this thesis entitled: “Study of Fe Doped Induced Effects on Physical Properties of CuO Nanostructures” by Asghar Ali bearing Registration No. 152-FBAS/MSPHY/S13 and in our opinion, it is fully adequate in scope and quality for the degree of MS Physics.


Committee

Dr. Waqar Ahmad

(External Examiner)

Department of Physics,

CIIT Islamabad

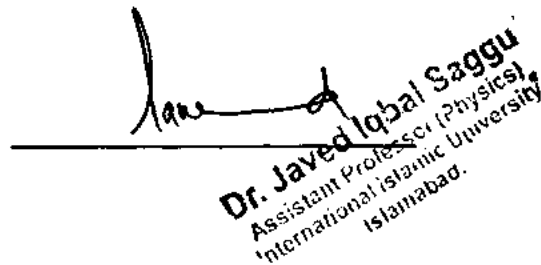


Dr. Javed Iqbal Saggi

(Supervisor)

Department of Physics,

International Islamic University Islamabad



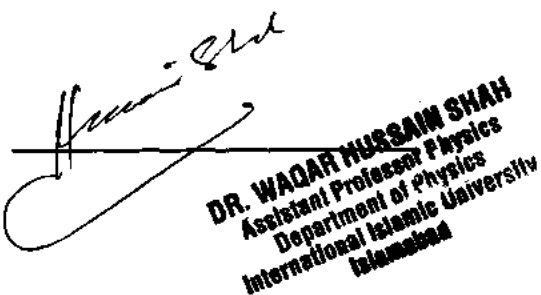
Dr. Javed Iqbal Saggi
Assistant Professor (Physics)
International Islamic University
Islamabad.

Dr. Waqar Shah

(Co Supervisor)

Department of Physics,

International Islamic University Islamabad



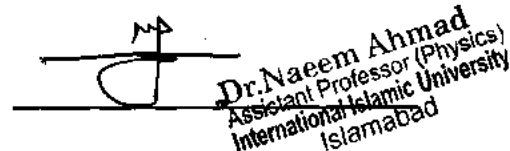
DR. WAQAR HUSSAIN SHAH
Assistant Professor Physics
Department of Physics
International Islamic University
Islamabad

Dr. Naeem Ahmad

(Internal Examiner)

Department of Physics,

International Islamic University Islamabad



Dr. Naeem Ahmad
Assistant Professor (Physics)
International Islamic University
Islamabad

بِسْمِ اللَّهِ الرَّحْمَنِ الرَّحِيمِ

Declaration of Originality

I hereby declare that the work contained in this thesis and the intellectual content of this thesis are the product of our own work. This thesis has not been previously published in any form nor does it contain any verbatim of the published resources which could be treated as infringement of the international copyright law.

I also declare that I do understand the terms of copyright and plagiarism and that in case of any copyright violation or plagiarism found in this work I Asghar Ali will be held fully responsible of the consequences of any such violation. The plagiarism report via turnitin ID: 553860992 is carried out and similarity index is 10%.

Signature. 

Name: Asghar Ali

Reg. No: 152-FBAS/MSPHY/S13

Dedicated to
My Beloved Parents
And
Respected Teachers

Acknowledgments

Praise is to the One, the Almighty, the merciful and the beneficent **Allah**, who is the source of all knowledge and wisdom, taught us what we knew not. We offer our humblest thank to the holy Prophet (**Peace be Upon Him**) who is forever a model of guidance and knowledge for humanity.

I am highly indebted to my affectionate supervisor **Dr. Javed Iqbal Saggu** for his inspiring guidance, remarkable suggestions, constant encouragement, constructive criticism and co-operation during our project work. Without his support and guidance, this report could not have been possible.

I am also grateful to all my friends and class fellows for giving me encouragement, appreciation and helping in completing this project.

Asghar Ali

List of Figures

Figure 1.1 The typical band structure of a) metals b) insulators and c) semiconductors.....	5
Figure 1.2 Illustration of super-exchange between two Mn atoms through Oxygen atom.....	7
Figure 1.3 Antiparallel alignment for small interatomic distances.....	8
Figure 1.4 Parallel alignment for larger interatomic distances	8
Figure 1.5 Quantum dots overview	9
Figure 1.6 Carbon Nanotubes	11
Figure 1.7 Crystal structure with large dark spheres to represent Cu and small light spheres for oxygen.....	13
Figure 2.1 A scheme of Top down approach	17
Figure 2.2 Bottom up approach scheme	18
Figure 2.3 A typical schematic of synthetic of CuO nanostructures by chemical precipitation	18
Figure 2.4 Hydrothermal synthesis of CuO nanostructures.....	21
Figure 3.1 An image of operational XRD.....	22
Figure 3.2 Diffraction from atomic planes.....	23
Figure 3.3 Working principle and schematic of XRD machine.....	24
Figure 3.4 Schematic of major parts of SEM	25
Figure 3.5 Schematic for working of SEM.....	25
Figure 3.6 Working principle of FTIR	27
Figure 3.7 Operational UV Vis apparatus at lab.....	28
Figure 3.8 Main working scheme of UV Vis.....	29
Figure 4.1 XRD plots of Fe doped and undoped CuO.....	31
Figure 4.2 SEM images of undoped CuO	34
Figure 4.3 SEM images of 1% Fe doped CuO	34

Figure 4.4 SEM images of 5% Fe doped CuO	35
Figure 4.5 SEM images of 7%Fe doped CuO samples.....	35
Figure 4.6 EDS spectrum of undoped CuO	36
Figure 4.7 EDS spectrum of 1% Fe doped CuO.....	37
Figure 4.8 EDS spectrum of 3 % Fe doped CuO.....	37
Figure 4.9 EDS spectrum of 5% Fe doped CuO.....	38
Figure 4.10 EDS spectrum of 7% Fe doped CuO.....	38
Figure 4.11 FTIR combined spectra for both doped and undoped CuO.....	39
Figure 4.12 (a ,b) DRS spectra of undoped CuO and 1% Fe doped CuO nanostructures	40
Figure 4.13 (a, b) DRS spectra of 3% and 5% Fe doped CuO nanostructures	41
Figure 4.14 (e) DRS spectrum of 7% Fe doped CuO nanostructures	41

List of Tables

Table 1.1 3d, 4d and 5d transition metals and their electron configurations	2
Table 1.2 Basic information of CuO.....	14
Table 2.1 Historic background of hydrothermal method	19
Table 4.1 Crystallite size of undoped and 1%, 3%, 5%, 7%, and 10% Fe doped.....	33
Table 4.2 Estimated band gap for undoped and Fe doped CuO samples.....	42

Table of Contents

Chapter No. 01	1
Introduction.....	1
1.1 Diluted Magnetic Semiconductors (DMSs).....	1
1.1.1 History of DMSs.....	1
1.1.2 Explanation of DMSs.....	1
1.1.3 Properties of DMSs.....	3
1.1.4 Applications of DMSs.....	3
1.1.5 Applications in Spintronics.....	4
1.2 Energy Band Theory	4
1.3 Ferromagnetism in DMSs.....	5
1.4 Origin of Ferromagnetism.....	6
1.4.1 Indirect Exchange Interaction.....	6
1.4.2 Super Exchange Interaction.....	6
1.4.3 Direct Exchange Interaction.....	7
1.4.4 Carriers Mediated Exchange Interaction.....	8
1.5 Nanostructured Materials.....	8
1.5.1 Types of Nanomaterials.....	9
1.5.1a Zero Dimensional Materials.....	9
1.5.1b One Dimensional Nanostructures.....	10
1.5.1c Two Dimensional Nanostructures.....	11

1.6 Cupric Oxide (CuO).....	12
1.6.1 Crystal Structure.....	12
1.6.2 Applications of CuO Nanostructures.....	13
1.6.3 Novel Application in LiBs.....	13
1.6.3 Some Basic Information of CuO at Room Temperature.....	14
1.7 Aim and Objectives.....	15
Chapter No. 02	16
Synthesis of Nanostructures.....	16
2.1 Synthesis Methodology of Nanostructures	16
1.2.1 Top Down Approach.....	16
1.2.2 Bottom up Approach.....	17
2.2 Co-precipitation Method	18
2.3 Hydrothermal Method.....	19
2.3.1 History.....	19
2.3.2 Significance.....	20
2.4 Synthesis of CuO Nanostructures	20
Chapter No. 03	22
Characterization Techniques.....	22
3.1 X-ray Diffraction (XRD)	22
3.1.1 Introduction.....	22
3.1.2 Working Principle.....	23

3.1.3 Bragg's Law.....	23
3.1.4 Advantages.....	24
3.2 Scanning Electron Microscopy (SEM).....	24
3.2.1 Introduction.....	24
3.2.2 Working Principle.....	25
3.2.3 Operating Conditions.....	26
3.2.4 Advantages of SEM.....	26
3.3 Energy Dispersive X-ray Spectroscopy.....	26
3.3.1 Working Principle.....	26
3.4 Fourier Transform Infrared Spectroscopy.....	27
3.4.1 Introduction.....	27
3.4.2 Working Principle.....	27
3.4.3 Sample Analysis.....	27
3.5 Ultraviolet Visible Spectroscopy (UV).....	28
3.5.1 Introduction.....	28
3.5.2 Samples Treatment.....	29
3.5.2a Transition Metal Treatment.....	29
3.5.2b Inorganic Compounds Study.....	29
3.6 Future Work.....	30
Chapter No. 04.....	31
Results and Discussions.....	31

4.1 Structural Analysis.....	31
4.2 Morphological Investigation.....	33
4.3 Chemical Analysis	36
4.4 Fourier Transform Infrared Spectroscopy (FTIR).....	39
4.5 Optical Properties.....	40
Conclusions.....	43
References.....	44
Plagiarism Report.....	48

Abstract

Metal oxides specially diluted magnetic oxides have unique size and dimensionally dependent chemical and physical properties and therefore have achieved too much attraction of researchers as a key components in devices for applications in the future.

The Cupric oxide (CuO) nanostructures also has interesting properties and attractive applications in Lithium ion batteries, photodetectors, super capacitors, energetic materials, gas sensors, solar cells and spintronics devices. The undoped CuO and Fe doped CuO nanostructures with different stoichiometric ratio have been synthesized via simple hydrothermal method. The prepared samples have been characterized using different advanced characterization techniques like X-rays Diffraction (XRD), Scanning Electron Microscopy (SEM), Energy Dispersive Spectroscopy (EDS) Fourier Transform Infrared Spectroscopy (FTIR) and Diffuse reflectance Ultraviolet Visible Spectroscopy (DRS). The XRD plots have established the successful synthesis of monoclinic structure and also confirm the incorporation of Fe ions in the cupric oxide crystal lattice by subjugating the Cu ions. The morphology is observed to be diverse from agglomerated particles to leaf like and rice like nanoparticles. The FTIR spectra patterns also display the monoclinic structure and fully support the XRD results. The diffuse reflectance visible spectroscopy have been used for bandgap calculation which is found to be 2.63 eV for undoped CuO and enhanced to 2.74-2.81 eV for Fe doped CuO nanostructures. This tailoring in band gap makes this material potential in different optical nanodevices.

Chapter No. 01

Introduction

1.1 Diluted Magnetic Semiconductors (DMSs)

If low concentration of magnetic ions is incorporated to a compound or alloy such alloy or compound is named as diluted magnetic semiconductor (DMSs). This is the type of semiconducting materials in which a sizable ion is replaced by a rare or transition metal ion which leads them to a number of cooperative effects. DMSs have attracted significant concentration of researchers due to their probable applications in spintronic devices [1].

1.1.1 History of DMSs

In 1970s, DMSs were first time introduced and the idea was further confirmed in 1980s when significant work was dedicated to this family of semiconductors of group II-VI. Later on, many experts suggested that the presence of small percentage of magnetic impurities in host matrix can cause a significant change in magnetic moments of host matrix without altering its optical, electrical and structural properties [2]. In 1996 at the Toho Ku University, Hideo Ohno's group measured the ferromagnetic ordering with 110K as Curie temperature in GaMnAs compounds.

1.1.2 Explanation of DMSs

The diluted magnetic semiconductor is a magnetic material with low/light concentration. The Curie temperature (T_c) of these material was high due to concentration of p-type charge carriers. The 3d transition metals are normally used for the production of DMSs because their 3d shells are partially filled. According to Hund's rule, 3d shells are filled parallel up to half filling by first five electrons therefore spin and magnetic moment are sizeable. Manganese (Mn) has a spin $S=5/2$. Configuration of most of transition metals is $4s^2$ which

makes these isovalent in II-VI compounds. For Zn its 3d shell is fully complete so it has no net spin.

Table 1.1 3d, 4d and 5d transition metals and their electronic configurations [3]

Sc ²¹	Ti ²²	V ²³	Cr ²⁴	Mn ²⁵	Fe ²⁶
3d	3d ²	3d ³	3d ⁵	3d ⁵	3d ⁶
4s ²	4s ²	4s ²	4s	4s ²	4s ²
Mo ⁴²	Tc ⁴³	Ru ⁴⁴	Rh ⁴⁵	Pd ⁴⁶	Ag ⁴⁷
4d ⁵	4d ⁶	4d ⁷	4d ⁸	4d ¹⁰	4d ¹⁰
5s	5s	5s	5s		5s
Cd ⁴⁸	La ⁵⁷	Hf ⁷²	Ta ⁷³	W ⁷⁴	Re ⁷⁵
4d ¹⁰	5d	5d ²	5d ³	5d ⁴	5d ⁵
5s ²	6s ²	6s ²	6s ²	6s ²	6s ²
Os ⁷⁶	Ir ⁷⁷	Pt ⁷⁸	Au ⁷⁹	Hg ⁸⁰	
5d ⁶	5d ⁷	5d ⁹	5d ¹⁰	5d ¹⁰	
6s ²	6s ²	6s	6s	6s ²	

The transition metals in which 3d electrons are less than 10, their successive electrons fill the 3d states in order defined by the competition between the Coulomb energy and crystal field energy. Cost of putting two electrons in the same orbital will have pairing energy. Here two cases of field are distinguished. Lower field case in which pairing energy is higher than the crystal field and in this case all of the electrons first singly occupy each orbital and then the orbitals are doubly occupied. When the crystal field becomes greater than pairing energy then electrons occupy all lower energy states which is known as strong field case [4]. The physical properties of DMSs can be described on the bases of two basic aspects. Generally spin dependent properties such as crystallographic electrical and optical properties of DMSs are similar to partial nonmagnetic compounds. When partial replacement of cat ion with magnetic ion takes place in binaries it leads to composition dependent variation in all properties of

materials like fundamental energy gap, similar to NMS in ternaries. However Hg in HgTe and Gd in GdTe are responsible for widening the band gap remarkably. The lead salts also show same effect. The spin independent properties of DMSs are functional in infrared detector applications [5].

1.1.3 Properties of DMSs

DMSs are fabricated by magnetic impurities such as Mn, Fe and Co etc. in the host matrix of semiconductors. The basic DMSs properties depend upon the host material. For example the manganese plays an important dual role in the semiconductors of group III-V such as GaAs. It provides localized spin because of its partially filled *d* shell and also behaves as acceptor. Mn^{2+} state of manganese exists in GaAs [6-7].

DMSs can be utilized as spin polarized carriers for storage of data. The possibility of using the electron's dual nature (spin along with charge) in the field of IT has played a significant role in the new field of spintronic. DMSs created by the doping of magnetic ions e.g., Mn, Fe, or Co can be used as spin-polarized carriers for data storage. At low temperatures, the interaction among these spins leads to ferromagnetic ordering. This ordering is necessary to create the spin-polarized carriers [12].

The chemistry of DMSs can be understood by doping a magnetic ions into semiconducting host matrix. The choice of material is very important because the fundamental properties of DMSs can be determined by the category of host semiconducting materials. For III-V semiconductors (GaAs), Mn dopant plays a double role. It plays the role of acceptor as well as provides a restricted spin. This happens due to its incompletely filled *d* shell. As Mn is an acceptor so it is a p-type material with Mn^{2+} oxidation state in GaAs.

1.1.4 Applications of DMSs

DMSs are auspicious because of their applications in science and technology. DMSs have gained significant attraction due to their applications in spintronic devices.

1.1.5 Applications in Spintronics

Spintronics has become an important field of research for the study of new semiconductor devices. Recently, DMSs have gained great interest due to functional applications in spintronic devices. These newly generated devices have many advantages over conventional semiconducting devices such as lower consumption of power, data processing at high speed and increased integration densities [7-11].

In addition to charge, the spin degree of freedom is exerted in the electrons. The integration of ferromagnetic elements into semiconductor devices, and the assimilation of data processing and magnetic storage on a single chip may be allowed by spin degree of freedom. The interference of quantum mechanical effects in devices can eventually lead it into designing of quantum computer [12].

1.2 Energy Band Theory

The orbiting electrons of atoms feel strong attraction from its nucleus. When they circulate around nucleus they possess different energy levels due to their separate energy levels. However in case of formation of solids, the energy levels of each and every atom split into their sublevels known as energy states. In solids, the forces are exerted by atoms on each other resulting in formation of distinguishable energy states but due to strict spacing they seem to form continuous energy bands. The electrons in outermost shell of atom are known as valance electrons and the band that they occupy is termed as valance band. This band is in some elements completely filled and sometimes has minimum number of electrons.

A band lies above the valance band in which electrons are free to move for the process of conduction is known as conduction band. There is a wide range of energy states in between two continuous admissible energy bands which is not filled by electrons. It is called as forbidden energy states and the difference of energy between them is called forbidden energy gap.

At ambient temperature semiconductors have

- a) The width of forbidden energy gap is of the order of 1 eV
- b) Incompletely filled conduction band
- c) Incompletely filled valence band

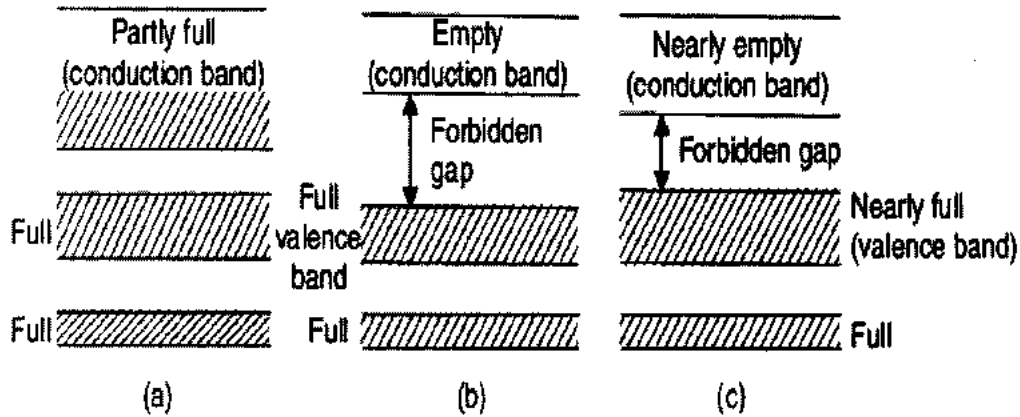


Figure 1.1 Typical band structure of a) metals b) insulators and c) semiconductors [13]

The behavior of semiconductor is insulators like at very low temperature i.e. of few mK because VB is completely filled and CB is empty. With a slight increase in temperature, the electron from VB jumps to CB creating vacancies in VB called holes. At room temperature, the behavior of many crystal is semiconducting which a proof of their dependence upon temperature is as well.

1.3 Ferromagnetism in DMSs

When magnetic moments are aligned in one direction then the spontaneous magnetization is known as ferromagnetism (FM) as a result domains are created by this alignment. This behavior strictly depends upon temperature and exists below a specific temperature called Curie-temperature (T_c) and above this temperature the orientation of moments is disturbed resulting in zero magnetization called paramagnetic state. The FM of DMSs is reported by different researchers [14-16]. Some of them also reported the room

temperature ferromagnetism in DMSs like GaMnP [17], GaMnN [18], GaMnSb [19] and GeMn [20].

This ferromagnetic property arises due to the presence of carriers in the semiconductors host matrix which shows an important feature of DMSs. So, increasing or diminishing the carrier's concentration can lead to an increase or decrease in magnetic order and helpful to understand optical control of magnetic behavior [21].

1.4 Origin of Ferromagnetism

The origin of ferromagnetism in DMSs is still not clear and appears as a big challenge however some reports show that it may be due to the exchange interactions [22-24].

1.4.1 Indirect Exchange Interaction

This type of interaction is raised when magnetic spins are coupled with each other at very large distances. In metals, this mechanism is strongly exhibited and for this case overlapping of ions is missing. In such interaction, a nonmagnetic anion like oxygen is situated at line which joins the magnetic ions. Because magnetic ions interact through some non-magnetic ions instead of direct contact with each other therefore it is termed as indirect interaction. Consequently in numerous magnetic materials, it is very significant to take into account the nature of indirect exchange interactions.

1.4.2 Super Exchange Interaction

The interaction which appears between non neighboring magnetic ions when they are linked with each other by a nonmagnetic ions positioned between them is super exchange interaction. Super exchange is said to be present in the antiferromagnetic compounds (such as NiO, MnO etc.). In the structure of MnO, Mn^{2+} ions that form FCC structure are diffused by another FCC structure of O^{2-} . In this situation Mn^{2+} ions are arranged as next nearest neighbors having antiparallel spin. An anion of O^{2-} is situated at midpoint of line joining these second

neighbors. The direct interaction amongst these two points is not very strong as observed. Thus this significant interaction is through the anion raised through p-state outer electrons of Oxygen. The expansion of p-wave function is outward from an anion in opposing lobes. Each lobe combine to form the total of one electron per anion. The spin of two electrons of lobes satisfies the Pauli Exclusion Principle. The lobes of d electrons of each Mn^{2+} cations are overlapped and mixed by these lobes. Only mixing of those lobes is possible which have same spins. This covalent mixing is similar to type of mixing which is responsible of binding mechanism of many semiconducting solids. The total energy is lowered by this method because Mn^{2+} cations on each side are oppositely oriented. This provides a driving force towards anti ferromagnetism. This is strong next to the line containing the anion [25].

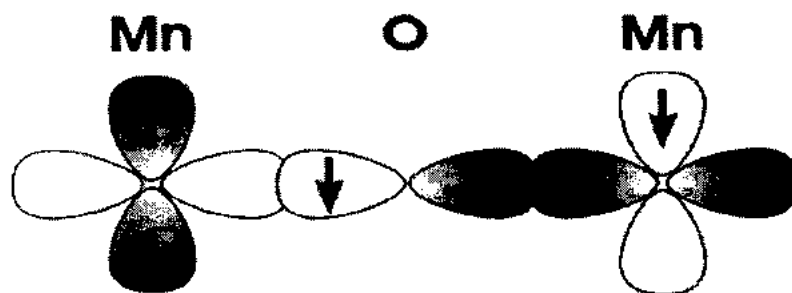


Figure 1.2 Illustration of super-exchange between two Mn atoms through Oxygen atom [26]

1.4.3 Direct Exchange Interaction

The case in which electrons on nearest magnetic atoms interact via an exchange interaction is known as direct exchange interaction. The exchange interaction is a quantum mechanical effect. Wave functions of neighboring magnetic moments have overlapping with each other and resulting in short range interaction. The separation of ions in this coupling shifts down quickly. Consider two atoms with one electron in each to understand the mechanism of direct exchange. When atoms are placed close to each other, the coulombic interaction becomes low and this causes electron to spend more time in the nuclei. Because this happens if electrons

lie in the same state but QM restricts the electrons to have reverse spins. Thus electrons get aligned with opposite spin giving rise to negative exchange, as in antiferromagnetism.

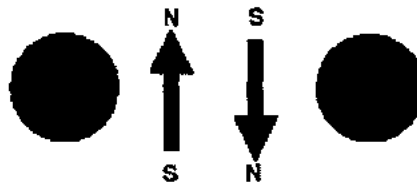


Figure 1.3 Antiparallel alignment for small interatomic distances [27]

However when the atoms are at larger distances, parallel alignment or positive exchange interaction (ferromagnetic behavior) occurs.

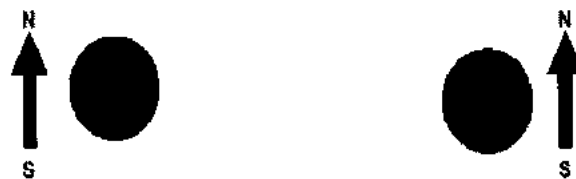


Figure 1.4 Parallel alignment for larger interatomic distances [27]

1.4.4 Carriers Mediated Exchange Interaction

This exchange addresses the interactions between the localized magnetic moments. This takes place by free electrons that exist in the system. In DMSs, spins of dopant magnetic ions are joined with the spins of either electrons or holes of the host. This behavior of DMS establishes a link between the electrical and magnetic properties of the material which is very much potential for their applications in spintronic devices.

1.5 Nanostructured Materials

The important family of materials for which the size of at least one dimension lies in the range of 1-100nm [28]. Such type of materials can have all three, two or at least one dimensions in the mentioned range.

1.5 1 Types of Nanomaterials

There are three major types of nanomaterials.

(a) Zero Dimensional Materials

(b) One Dimensional Materials

(c) Two Dimensional Materials

1.5.1a Zero Dimensional Materials

“The materials exhibiting quantum confinement in all three dimensions”. Examples are quantum spheres, quantum dots and nanoparticles.

Quantum dots are materials which are less than 10 nm in size and are zero dimensional. These are nano crystals of semiconducting material that are small enough to exhibit quantum mechanical properties. Quantum dots are the units that contain a small droplet of free electrons. Usually in quantum dots the size, shape and number are controlled their confinement is just like quantum confinement in atom 3D spatial dimensions [29].

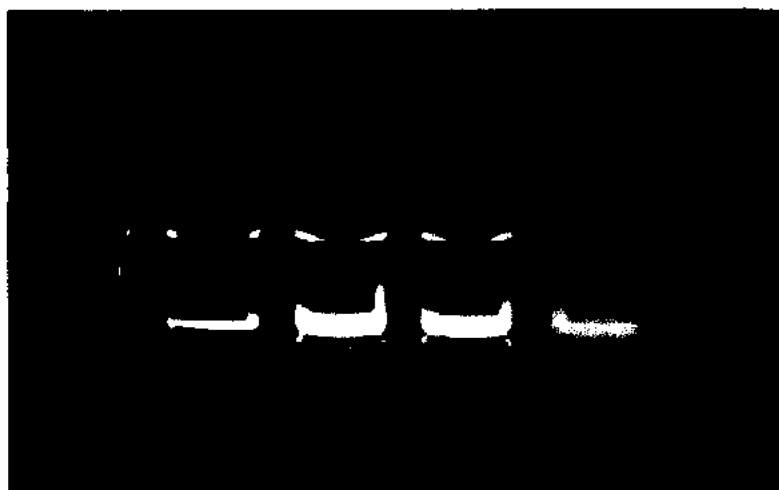


Figure 1.5 Quantum dots overview [30]

These were first discovered by Alexey Ekimov in 1981 and then used. In quantum dots even a small disturbance generated in the system either escape of electron can cause a huge change in the system. The characteristics of quantum dots are related to shape and size. These are significantly changed with and change with a significant change in the size and shape.

For example, band gap of quantum dots is inversely proportional to their size. An increase in frequency of emitted light can be noted as the size of the quantum dot decreases. In fluorescent dye applications also the color of the dots shows a shift from red to blue as the particle size is made smaller and smaller. They are produced by colloidal synthesis, fabrication and viral assembly and their size may be controlled at the time of formation which makes these conductive properties in controlled range. Quantum dots are used in computing photovoltaic cell, LEDs, Light emitting devices and biology and medicine.

1.5.1b One Dimensional Nanostructures

The materials which have at least two dimensions between 1 and 100 nm. Examples are nanotubes, nanorods, nanobelts and nanowires. Nanotubes are the tubes in which diameter is at nano scale. Carbon nanotubes are most important in this group. These tubes were first time discovered in fullerene in 1991 by Sumio Iijima and were named as carbon nanotubes. Carbon nanotubes are mostly found in two types i.e. Single walled carbon nanotubes (SWCNTs) and Multi walled carbon nanotubes (MWCNTs). A single wall carbon nanotube is achieved by rolling a sheet of graphene (a single layer of graphite having size in nanometres) into a cylinder. Typical diameter of SWCNTs is in the range of 0.7-1.4 nm and their length may be in several micrometres. The catalytic iron nanoparticles synthesized within protein cages as catalysts have been used to develop single walled carbon nanotubes (SWNTs).

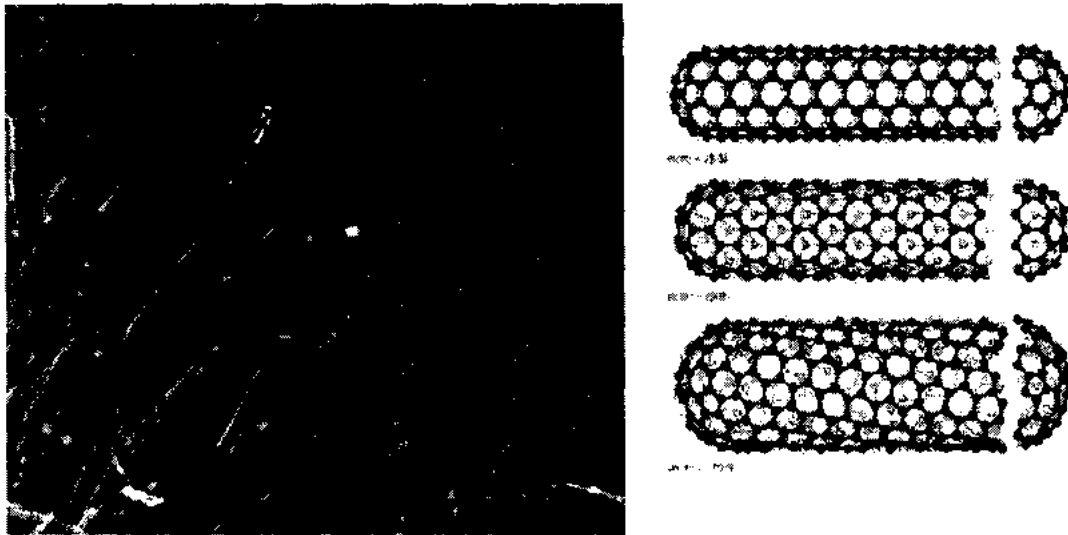


Figure 1.6 Carbon Nanotubes [31]

The carbon nanotubes may be multi walled if they have their shape consisting of multi walls of carbon (MWCNTs) are composed of several coaxial multiwall tubes. CNT's are unique nanostructures with significant mechanical and electronic properties, some of which are due to close relation between carbon nanotube and graphite and some for their 1 D aspect. CNT's also exhibit good nano mechanical properties due to high Bongs modulus. The modulus of SWCNTSs (1210 Gpa) and multi walled MWCNTSs (1260 Gpa) are very high. In comparison, the metallic wires such as copper and steel have a modulus of only 200G pa.

1.5.1c Two Dimensional Nanostructures

The type of materials having at least one dimension in the range of nanometer. Thin films are its good example which may be crystalline, polycrystalline or amorphous nature and can be found in the two main hydrophilic (water absorbent) or hydrophobic (water repellent). Scattering of light is less for their small structure and vice versa. The other examples of 2-D are nanosheets, nanoplates, nanofilms and nanolayers.

1.6 Cupric Oxide (CuO)

Nanostructured transition metal oxides is an important class of nanomaterials and in contestable part of development of other materials [32]. These materials have been achieving much attraction because of their properties and applications in numerous fields [33-34]. The physical and chemical properties of MOs arise because of their sizes, structures, shapes and compositions of nanostructures. The phenomenon like increase in surface to volume ratio, quantum confinement effects and increase in surface energy are observed after their conversion to nanoscale [35-37].

In the family of transition MOs, the cupric oxide (CuO) has been an important topic of research because of low cost and nontoxic as well as its significant properties as p type semiconductor with narrow direct band gap (1.2 eV at bulk) and also superconductive and magneto resistance materials [38,39]. In addition to these properties CuO is an important material for selective solar absorbance and low thermal emittance [40]. Cu^{2+} ions in CuO play an important role in Cu based superconductors. Physical properties such as high temperature superconductivity, spin dynamics and electron correlation effects are also reported. CuO nanoparticles exhibit antimicrobial activity against Gram positive and Gram negative if these are coated onto the fabrics. [41].

1.6.1 Crystal Structure

Cupric oxide CuO has monoclinic crystal structure of space group $c/2$ with lattice parameters $a=4.6837\text{\AA}$, $b=3.4226\text{\AA}$, $c=5.1258\text{\AA}$, $\alpha=\gamma=90^\circ$ and $\beta=99.9^\circ$ [42-43].

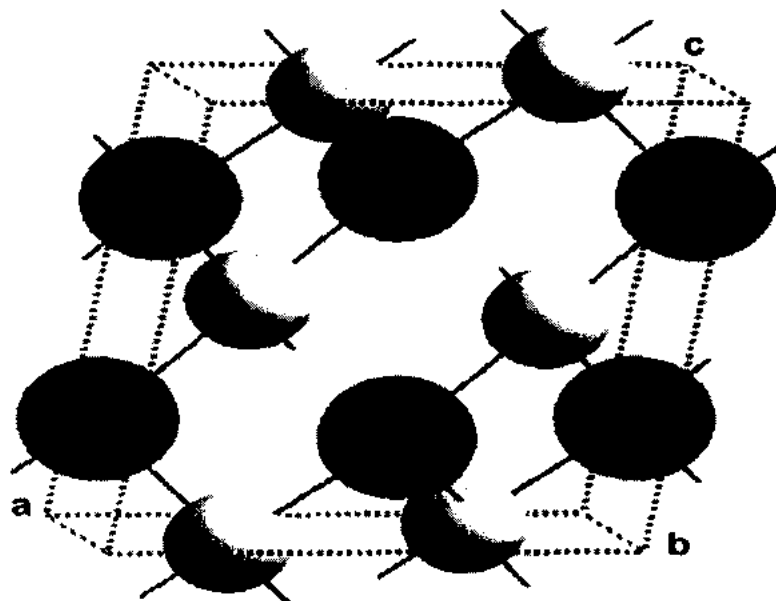


Figure 1.7 Crystal structure with large dark spheres to represent Cu and small light spheres for oxygen [43]

1.6.2 Applications of CuO Nanostructures

The CuO nanomaterials are used in lithium batteries (LiBs) due to high theoretical capacity [44] due to their high carrier concentration, high solar absorbance, relatively low thermal emittance and good electrical properties. They are also promising materials for the fabrication of solar cells [45]. In many applications CuO nanostructures are widely used e.g. photodetectors [46], energetic materials (EMs) [47], nanofluid [48] bio-sensors [49], gas sensors [50], removal of inorganic pollutants[51,52], super capacitors [53], photo catalysis [54], field emissions[55] and as magnetic storage media with doping of magnetic impurity [56].

1.6.3 Novel Application in LiBs

Transition MOs with nano size can be considered as anode of LiBs because of the tremendous cycling and theoretical capacities [57-60]. CuO is very important in MOs for LiBs as it has 670 mA h/g theoretic capacity, environmental goodwill, and lower cost and easy to produce as compared to others [61-62]. The variation in volume at the time of lithium uptake process is drawback of CuO in addition to important properties that restricts its use as LiBs.

This drawback discussed earlier causes mechanical strain resulting in rapid capacity decay [61,62]. Although this strain has been reduced by synthesizing diverse morphology of CuO nanostructures like nanorods [63], 0D nanoparticles [64] and 2D/3D hollow nanostructures [62,57]. Various methods are also used to enhance their electrochemical performance. Among these synthesized nanostructures, hollow CuO nanostructures have been selected for LiBs because of surface permeability, high surface area and lower material density [62,65].

1.6.3 Some Basic Information of CuO at Room Temperature [66]

Table 1.2 Basic information of CuO

Molecular formula	CuO
Molar Mass	79.57 g/mol
Appearance	Black to brown powder
Density	6.31g/cm ³
Melting point	1200 ^o c
Refractive index	1.4
Band gap	1.2eV (direct)
Hole effective mass	0.24m _o
Hole mobility	0.1-10 cm ² /Vs
Dielectric constant	18.1
Cell volume	81.08 Å
Cell contents	4 [CuO]

1.7 Aim and Objectives

Metal oxides semiconductors have become very important due to their various properties which depend upon synthesis parameters such as surfactants, precursors, temperature, time duration and pH value. The particle size morphology and band gap of nanostructures can also be changed by adding dopant (Fe) impurities. Therefore undoped and Fe doped CuO nanostructures will be synthesized via simple hydrothermal method. The structural and physical properties will be tuned by Fe doping to make it potential for different applications such as optoelectronic nanodevices. The spin degree of freedom will make it potential for spintronics devices (future work).

Chapter No. 02

Synthesis of Nanostructures

2.1 Synthesis Methodology of Nanostructures

The progress of synthetic methods has become an important area for understanding and application of nanoscale materials. This makes the scientists able to modify different parameters such as particle size, morphology, size distribution and composition. The aim of nanotechnology is to deliver smaller and smaller devices based on the components having size approaching to size of atoms and molecules. The goal of nanotechnology is to fabricate the materials with at least one dimension in size less than 100 nm. When materials are reduced to nanoscale dimensions, the physical and chemical properties are greatly enhanced. These properties depend upon structure, size, shape, and composition of nanostructures. Many other interesting phenomena like surface energy and surface-to-volume ratio remarkably increase at nanoscale [67-69]. Numerous synthetic methods can be used but all the methods are based on two main approaches for nanofabrication e.g. top down approach and bottom up approach [70].

1.2.1 Top Down Approach

The type of approach in which the material is synthesized by breaking down into small parts. It begins from large picture and breaks it into small fragments. There are many synthetic techniques that are used to create nanostructures using top down approach such as lithography (photolithography, ion beam lithography, electron beam lithography), embossing, ball milling method and molding printing etc. Top down approach uses both conventional and nonconventional methods to fabricate nanostructures. Different industries use top down approaches e.g. semiconductor industry uses this technique to integrate chips for circuits; and

ceramics industry makes alloys by these techniques. In addition to advantages top down approach has few drawbacks.

- It is too much expensive due to clean rooms requirement.
- It has less commercial applications.
- It has big chance of impurity introduced at the time of fabrication.
- The products of top down approach are almost impure.

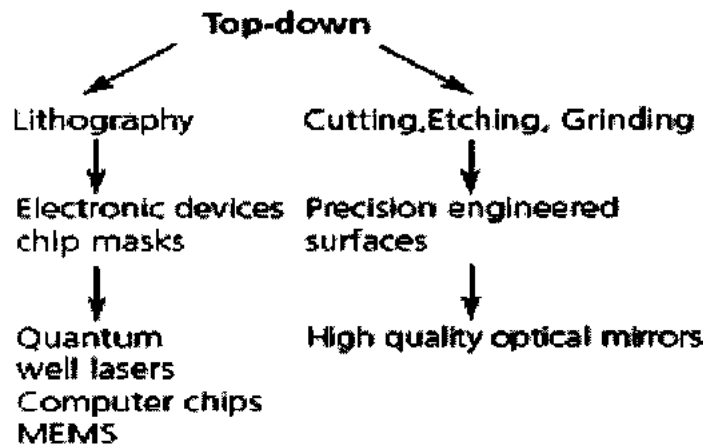


Figure 2.1 A scheme of top down approach [71]

2.1.2 Bottom up Approach

The type of approach in which the nanomaterials are synthesized by adding atoms and lattices to form clusters and nanostructures. The main idea of this approach is taken from natural phenomenon in which all the materials are designed from atoms, cells and crystals and also human beings from bottom up technique.

The main synthesis methods relating to bottom up approach for synthesizing nanostructures are chemical co precipitation method, sol-gel method, thermal evaporation method, carbo thermal method, solvothermal method, chemical aqueous method, hydrothermal method, physical vapor deposition (PVD) and chemical vapor deposition (CVD).

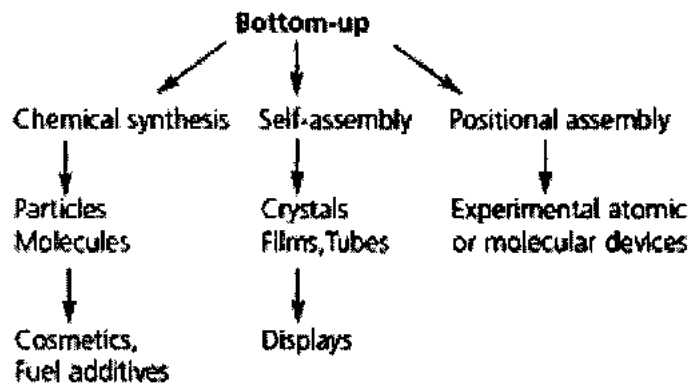


Figure 2.2 Bottom up approach scheme [71]

2.2 Co-precipitation Method

Co-precipitation technique is the easiest and the most useful technique for the synthesis of the nanostructures. In this technique, aqueous salt solutions of reactants are mixed to produce precipitation of insoluble substance by exceeding the solubility limit. High pH values are used where large production yields are expected [72].

The main advantage of co-precipitation method over all other method for the synthesis of CuO nanostructures are production of enough amount of material as it is simple and quick preparation, control of production rate and easy to control the composition and particle size. Various possibilities to improve the particle surface state and overall homogeneity. There is no need of extra mechanical heat treatment.

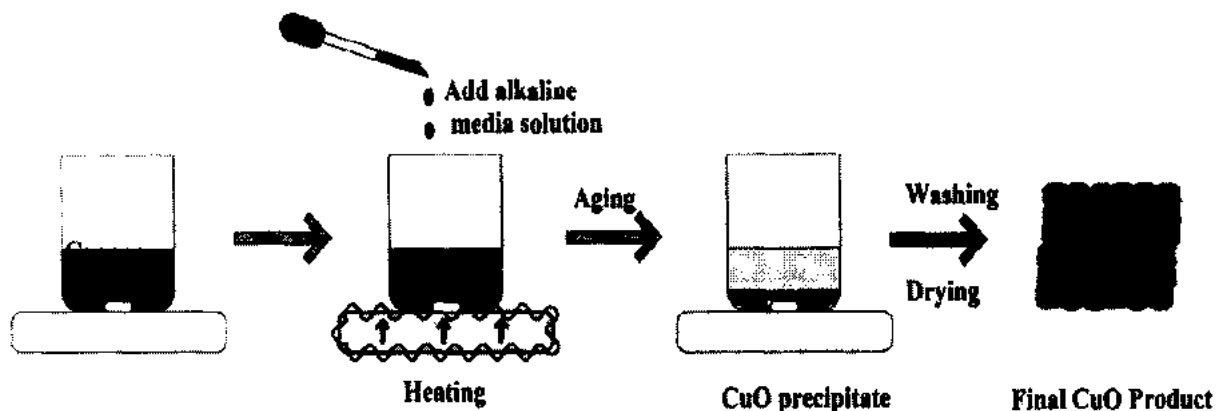


Figure 2.3 A typical Schematic of synthetic of CuO nanostructures by chemical precipitation [73]

2.3 Hydrothermal Method

2.3.1 History

The term hydrothermal was first used by Sir Roderick Murchison in the mid of 19th century. Initiative of publication was taken in reports in 1845 on hydrothermal method on the topic of synthesis of tiny quartz crystals by K F E. Scaftaul. Later on in France, Germany and Italy this method for the synthesis of minerals was started. Although the size of their products did not exceed thousands or hundredth of millimeter but their main objective was to create the natural conditions of pressure and temperature in the earth crust. The German, Switzerland, and Italian laboratories performed hydrothermal experiments using thick wall glass tubes to maintain the pressure and temperature. Historic background is summarized below

Table 2.1 Historic background of hydrothermal method [74]

Period	Focus	Equipment
1850-1900	Mineral synthesis	Simple reactors, Digesters etc.
1900-1940	Mineral synthesis improvement in Pt conditions	Morey autoclaves, Flat closures
1940-1950	Large size and large scale production of quartz, production of zeolites, clays, mica.	Test tube type welded closure
1950-1960	Phase diagram for natural synthesis	Morey, Tuttle. Closure
196—1970	Synthesis of new inorganic compounds	New designs from USSR
1970-1980	Materials synthesis and ceramic processing	Large autoclaves, new design pt conditions

1980-1990	Importance in material science and synthesis of chemical physical chemistry	
>1990	Age of solvo thermal physical chemistry through hydrothermal synthesis	Design of new reactors e g batch reactors

2.3.2 Significance

- Several inorganic salts can be well liquefied in water, depending on the requirements permit a very pliable adjustment of the source of the metal ions.
- Water is low-cost, non-toxic and environment friendly.
- To modulate the growth of the final nanocrystals small coordinating molecules can be easily applied and
- The oriented growth of nanocrystals may be favored by strong polarity of water [75].

2.4 Synthesis of CuO Nanostructures

The CuO nanostructures were prepared by simple hydrothermal method. The $\text{CuCl}_2 \cdot 2\text{H}_2\text{O}$ as a precursor Acetic Acid (CH_3COOH) as a capping agent and also for controlling particle size distribution and sodium hydroxide (NaOH) (which is a strong base) is used for a the adjustment of the pH value of the solution. Under constant heating and vigorous stirring the whole reaction occurred in distilled water.

To prepare 0.1M solution of $\text{CuCl}_2 \cdot 2\text{H}_2\text{O}$ was added to specific amount of distilled water in a beaker. By using magnetic stirrer then the solution was stirred for 10 min at 400rpm. Now to control the particle size and as capping agent, 2ml of acetic acid (CH_3COOH) was mixed in solution and was also stirred for 10min at 400 revolution per minute (rpm) rate. To maintain the pH value, now Sodium hydroxide (NaOH) was poured drop by drop in the reaction medium. The nucleation process started and precipitates were formed when pH reached nearly 8. After this the solution was left for 1hr heating at 500 revolution per minute at the temperature

of 100°C. By the passage of 1hr now the hot solution was shifted to 100ml autoclave and was placed in furnace for 24hrs at 150°C temperature. Next day the material was dried completely it were taken out from autoclave and centrifuged three times for 5 minutes each and centrifuged solution was again placed in furnace for overnight by setting 120 °C temperature. Finally the dried chemical was grinded to powder form. The doping process was also done by following the same procedure. The different stoichiometric ratios of $\text{CuCl}_2 \cdot 2\text{H}_2\text{O}$ and $\text{FeCl}_3 \cdot 6\text{H}_2\text{O}$ were used for desired composition of Fe dopant into host matrix. The flow chart of synthesis is shown in figure 2.4.

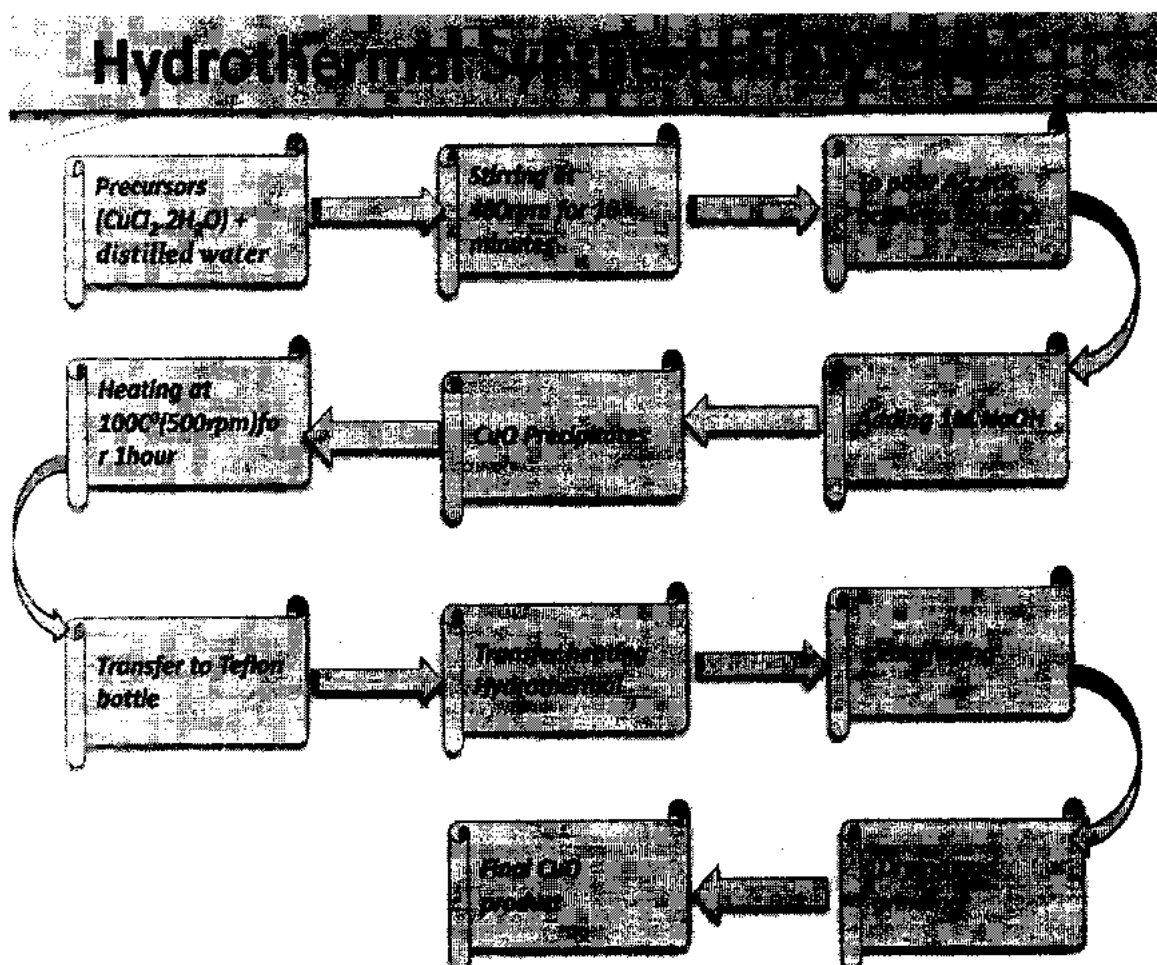


Figure 2.4 Hydrothermal synthesis of CuO nanostructures

Chapter No. 03

Characterization Techniques

The aim of chapter is to discuss briefly the techniques and their working principles used in experimental process for analyzing and characterizing the data. So, XRD, SEM, EDS, FTIR and UV visible spectroscopy will be discussed.

3.1 X-ray Diffraction (XRD)

3.1.1 Introduction

Most commonly XRD is used to test the crystal type and structure of materials. It is the best technique which justifies whether the material is crystalline or amorphous. The crystalline materials have specific interatomic distance between their layers approximately of order of 0.15 nm to 0.4 nm. When they are exposed to light of x-ray ranging from 3 eV to 8 eV, the separation between layers acts as a slit as a result diffraction through layers is observed. The diffracted rays may interfere constructively or destructively and final pattern is shown by computerized equipment.



Figure 3.1 An image of Operational XRD

3.1.2 Working Principle

The x-rays from a source are guided on the sample. These rays are diffracted from interatomic layers of crystals. The diffracted rays either interfere constructively or destructively resulting in final XRD pattern. The obtained pattern contains information about the phase and crystallinity of given sample. The condition of diffraction can be explained by Bragg's law.

3.1.3 Bragg's Law

According to Bragg "when a crystalline material is illuminated by a monochromatic light of wavelength (λ) it is scattered from the different layers of crystal plane ". The information are only given by rays interfering constructively.

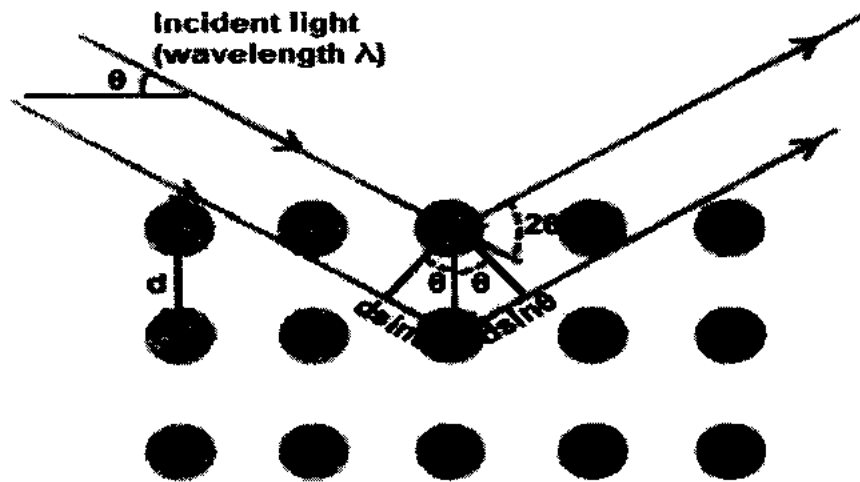


Figure 3.2 Diffraction from atomic planes [76]

The Bragg's equation is

$$n\lambda = 2d \sin\theta \dots\dots\dots(3.1)$$

Here n is order of grating,

d is separation between any two planes of crystal,

θ is Bragg's angle and λ is wavelength of x rays.

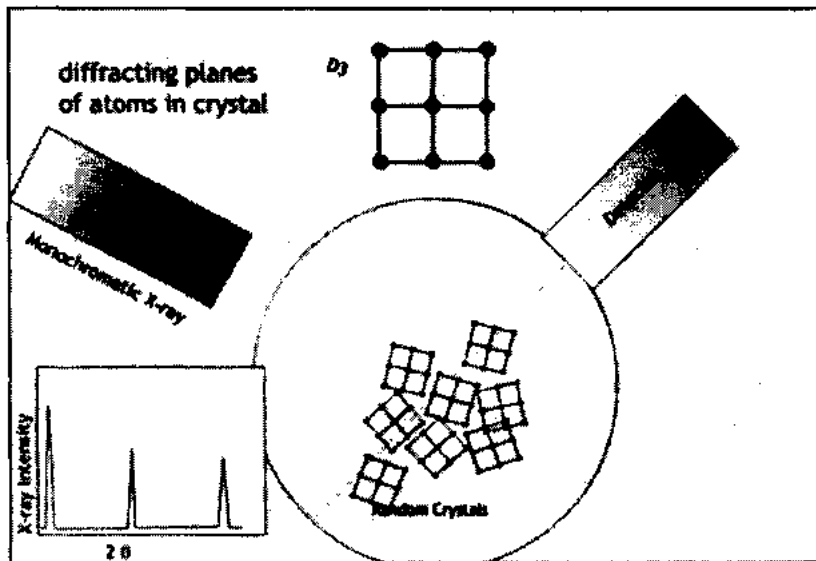


Figure 3.3: Working principle and schematic of XRD machine [76]

3.1.4 Advantages

X-ray diffraction technique is very multipurpose and having no destructive background. The main attraction of XRD is that it is useful for both bulk as well as nanostructured materials.

3.2 Scanning Electron Microscopy (SEM)

3.2.1 Introduction

The scanning electron microscopy (SEM) is one of the most multipurpose instruments available for chemical composition, characterization, examination and analysis of microstructure morphology. The resolution of 10nm and magnification of 5000 to 300000 X can be achieved by SEM. The schematic diagram of SEM is shown in figure 3.4

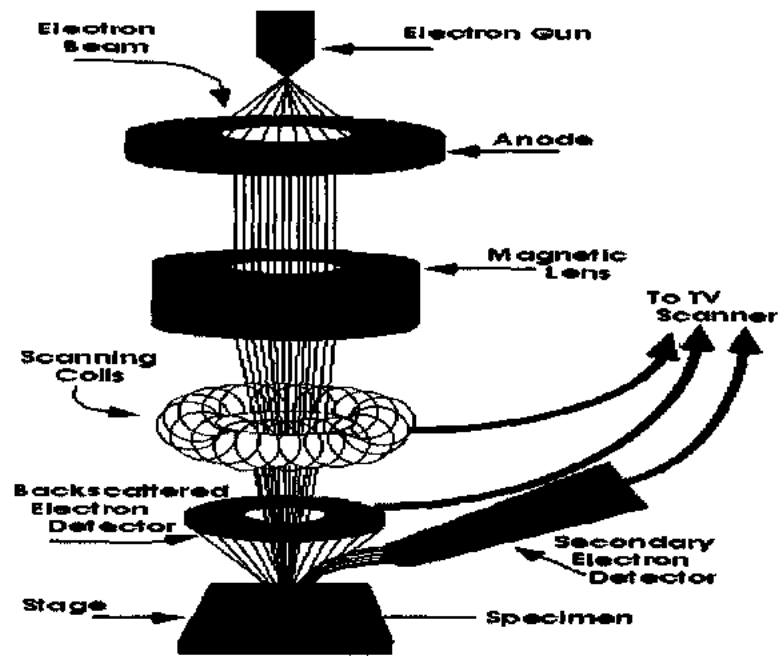


Figure 3.4 Schematic of major parts of SEM

3.2.2 Working Principle

When a beam of electron strikes the specimen it gets scattered and these scattered electrons are helpful in the formation of images of morphology of the sample. There are different types of signals which are radiated from the sample including back scattered electrons, secondary electrons, auger electrons, x-rays and cathode luminescence (light). The detector is present in the sample chamber detects these signals and shows through computer interface.

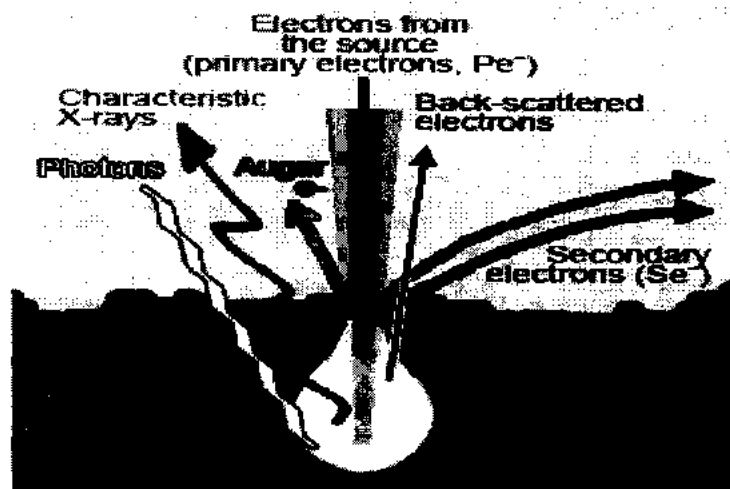


Figure 3.5 Schematic for working of SEM

3.2.3 Operating Conditions

In order to operate SEM it is necessary to produce vacuum inside the sample chamber. The wet sample should not be used to overcome vaporization effects. While using the samples of non-metals it must be covered by a thin layer of conducting material.

3.2.4 Advantages of SEM

Some advantages of SEM are as under. In addition to morphological investigation, the Chemical compositions and constituents in the sample can also be measured using EDS commonly attached with the SEM.

- Images at high resolution and magnification can be obtained.
- The crystalline phases of the specimen can be calculated by using it.

3.3 Energy Dispersive X-ray Spectroscopy

An analytic technique coupled with SEM, TEM or STEM EDS signals which is eligible to detect the X-rays released from the sample in the electron microscopy is known as Energy Dispersive X-ray Spectroscopy. By this Spectroscopy (EDS), the phases like elemental and Chemical can be characterized. In SEM, TEM or STEM more electrons are ejected as a result of bombarded the electrons on sample surface. Vacancies are created inside the atoms of sample so x rays spectra of different energies are detected. These spectra deliver information about chemical composition and constituents of sample. The information about the Sample composition from the energy of X- rays is measured [77].

3.3.1 Working Principle

When electron beam is made incident on sample these electrons knock out electrons from the innermost shell of sample's atoms. The vacancies of ejected electrons are filled by outer electrons. Their empty positions are filled by some other electrons called Auger

electrons and as a result x rays are produced that give information about the composition of the sample.

3.4 Fourier Transform Infrared Spectroscopy

3.4.1 Introduction

FTIR is an analytic technique which is used to measure the chemical purity and stretching modes in the materials. FTIR is the best way to check the vibrational modes of chemical bonds inside the samples. Because of variety of molecular vibration of stretching and bending different bonds respond to the infrared light is different. FTIR is based on the principle of Michelson Interferometer therefore less expensive than the other spectrometers.

3.4.2 Working Principle

When sample is illuminated by infrared light it absorbs this light. Due to internal interactions of light, a pattern of sample is obtained indicating the absorption bands. When sample is irradiated by infrared light then the light excites the atoms of samples which results in the pattern of atomic bonding. The schematic diagram is shown in figure 3.6.

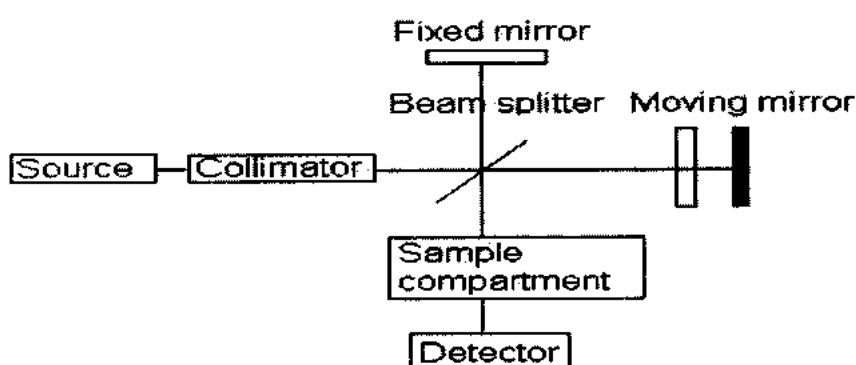


Figure 3.6 Working principle of FTIR [78]

3.4.3 Sample Analysis

The sample analysis by IR has basic steps as follows;

- (i) Black body is illuminated to emit infrared light (energy).
- (ii) Interferogram generates signals when light is introduced and ejected from the Interferometer.
- (iii) The beam interacts with surface in two ways either causing transmittance or reflection
- (iv) Finally the transmittance or reflection is detected in the chamber giving the final pattern of samples.

3.5 Ultraviolet Visible Spectroscopy (UV)

3.5.1 Introduction

In the UV visible regions if the spectroscopy of ultraviolet visible light is involved the spectroscopy is said to be ultraviolet visible spectroscopy. In the electromagnetic spectrum lying in the visible region, the molecule undergoes electronic transitions. The main use of UV is to determine the quantitative value of solutions of highly conjugated organic compounds and transition metal ions. The compounds are colored by some absorbance and the wavelength absorbed can be marked for specific compound.



Figure 3.7 Operational UV Vis apparatus at lab

Accession No. TH-14516

3.5.2 Samples Treatment

3.5.2a Transition Metal Treatment

When transition metals solution is treated light is absorbed in its color is changed because d electrons are shifted to excited state. The existence of other species, like the certain anions or ligands the color of metal ion solutions is strongly affected. For instance, the dilute solution of copper sulfate has very light blue color but by ammonia addition color is changed to the wavelength of maximum absorption (λ_{max}).

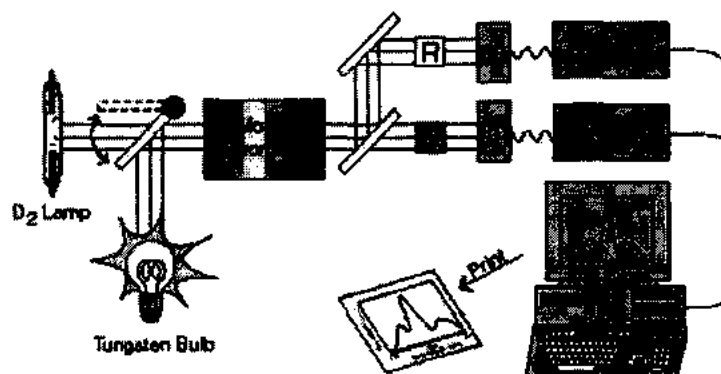


Figure 3.8 Main working scheme of UV Vis

3.5.2b Inorganic Compounds Study

Also the organic compounds absorb the light in the UV region and this absorption is especially for high degree conjugation compounds. Commonly ethanol for organic-soluble compounds, or water for water soluble compounds are used as solvents for all determinations. The pH and polarity of solvent can influence the absorption spectra. The transfer of charge gives rise to the colors are too intense and quantitative measurement can be done by these. According to the Beer-Lambert law, the absorbance and the concentration of a solution are directly proportional to each other. The concentration of a solution can be determined by UV/VIS spectroscopy. But necessarily one must know that how quickly concentration can change the absorbance.

We can take this from standard references (tables of molar extinction coefficients), or can measure more accurately from the calibration curve. The UV/V spectrometer is detector as well. The analyst presence shows a response that is considered to be proportional to concentration. For accuracy of results the instruments response might to be comparable with standard. The process has similarity with use of calibration curves. This comparison of particular concentration is known as response factor.

In a quantitative way the method is often used in solution to determine concentrations of an absorbing species using the Beer-Lambert law:

$$A = -\log_{10}(I/I_0) = \epsilon \cdot c \cdot L \dots \dots \dots (3.2)$$

Where A = the measured absorbance,

I_0 = the intensity of the incident light at a given wavelength,

ϵ = the molar absorptivity or extinction coefficient

I = the transmitted intensity,

c = the concentration of the absorbing species, and

L = the path length through the sample,

Here, ϵ is a constant at a particular temperature and pressure relating to fundamental molecular property in a given solvent having units of $l / M \times cm$ or often $AU / M \times cm$.

3.6 Future Work

As one aim of my work is to introduce the ferromagnetism in CuO and tuned its dielectric response. In future, magnetic and dielectric properties through VSM and LCR meter respectively will be measured of these samples.

Chapter No. 04

Results and Discussions

The structure of synthesized samples have been examined using XRD, morphological and chemical analyses of samples have been done using the SEM and EDS techniques. The aim of XRD is to check the crystallinity and phase purity. By SEM topography and grain size investigations are made and EDX spectroscopy is used to observe constituents of the prepared samples. The vibrational modes and the surface chemistry are analyzed by FTIR. Then DRS (UV) is adopted for finding the optical direct band gap of synthesized samples

4.1 Structural Analysis

In order to investigate the crystal structure and phase purity the XRD with x-ray Cu K α radiation ($\lambda = 1.5405\text{\AA}$) has been used at room temperature for undoped CuO and Fe doped CuO nanostructures in powdered form. The angle range 2θ and scan step size are taken in $10^\circ < \theta < 80^\circ$ and 0.01 respectively.

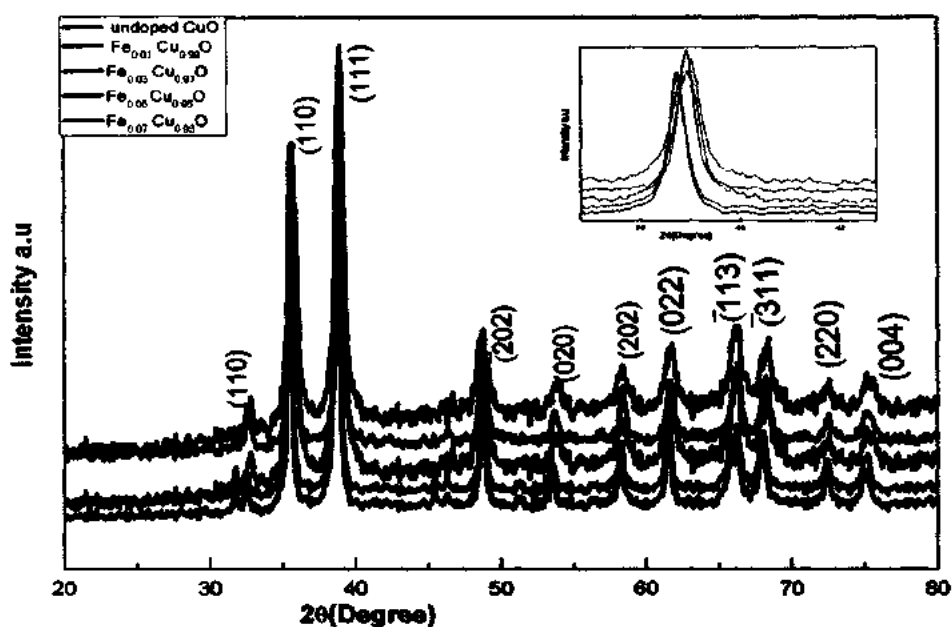


Figure 4.1 XRD plots of Fe doped and undoped CuO

Fig. 4.1 shows the XRD patterns of undoped as well as Fe doped CuO structures in which peaks are observed at 32.5305° , 35.4828° , 38.7256° , 48.7256° , 53.4827° , 58.3442° , 61.5154° , 66.2742° , 68.0991° , 72.4043° and 75.2167° corresponding to (110),(-1 11),(111),(-2 0 2),(020),(202),(-113),(-311), (220),(311) and (004) plane respectively. No clear change in peaks position are seen which indicates that the powder produce is of monoclinic phase and sharpness of peaks is identity of its high crystallinity. The careful study of diffraction peak reveals the absence of extra iron phase (iron oxides, metallic iron or any binary copper iron phases) in case of all Fe doped CuO products. Hence it means that doping is successful and Cu sites are filled with Fe ions without the generation of any effect on the crystal structure of host matrix CuO. This replacement of Cu^{+2} ions by Fe ions is as a result of unremarkable radii difference between Cu and Fe ions which are 0.73 Å, 0.64 Å and 0.74 Å for Cu^{2+} , Fe^{3+} and Fe^{2+} respectively. The Debye–Scherer equation is used to calculate the average crystallite size of undoped and Fe doped CuO at most intense diffraction peak (111) by finding its full-width at the half-maximum. The Debye formula is

$$D=0.9 \lambda/\beta \cos\theta.....(4.1)$$

Here D is average crystallite size, λ is (1.540 Å) and represents the wavelength of incident X ray beam, β is the peak width at half width maximum (FWHM) and θ is the Bragg diffraction angle. The average crystallite size of undoped CuO samples is 29.94nm and Fe doped CuO samples was found to be in between the range 17-25 nm as given in table 4.1. The table 4.1 gives the combined crystallite size of undoped 1%, 3%, 5%, and 7% Fe doped CuO samples. It is observed that crystallite size is higher for undoped CuO which is regularly decreased by adding Fe content up to 3% and then slowly increased with increase in dopant percentage in common trend for samples $\text{Fe}_{0.05} \text{Cu}_{0.95}\text{O}$ and also a small increase for $\text{Fe}_{0.07} \text{Cu}_{0.93}\text{O}$. It displays a decrease by doping initially up to 3.0 wt % Fe doped and then an increase in particle size. The crystallite size of samples is observed to decrease for samples $\text{Fe}_{0.01} \text{Cu}_{0.99}\text{O}$

and $\text{Fe}_{0.03}\text{Cu}_{0.97}\text{O}$ from 25.92 nm to 17.80 nm i.e. is minor as compared to the 0% doped sample. It is found in literature that when Fe is doped into some compounds like SnO_2 etc. the crystallite size decreases by doping [78-82]. This happens due to the fact that Fe^{3+} ions might be substituting the ions of Lattice because of their smaller cationic radius which causes decrease in crystallite size. Similar situation may be present in the case of 1.0-5.0 wt% Fe doped samples and Cu^{2+} (0.73 Å) ions may be replaced by Fe^{3+} (0.63 Å) ions which could be responsible of decrease in crystallite size. The crystallite size is also to be increasing via increasing the dopant concentration but still the average crystallite size is less than the pure CuO sample so there might be a possibility that few ions of Cu^{2+} being replaced by Fe^{3+} and some by Fe^{2+} ions. The continuous increase in particle size of Fe doped nanostructures is due to the increase in doping concentration [83].

Table 4.1 Crystallite size of undoped and 1%, 3%, 5%, 7%, and 10% Fe doped CuO

Sample	Reflection(2θ)	Spacing (d)	Crystallite size(nm)	(h k l)
Undoped CuO	38.7256	2.32526	29.94	(111)
$\text{Fe}_{0.01}\text{Cu}_{0.99}\text{O}$	38.9197	2.31411	25.92	(111)
$\text{Fe}_{0.05}\text{Cu}_{0.99}\text{O}$	38.8681	2.31707	22.25	(111)
$\text{Fe}_{0.07}\text{Cu}_{0.99}\text{O}$	38.713	2.32599	22.11	(111)

4.2 Morphological Investigation

In order to investigate the morphology the scanning electron microscopy (SEM) has been employed. The SEM images were taken at different resolutions (1µm to 500nm). The figs 4.2-4.5 show SEM images of undoped and Fe (1%, 3%, 5% and 7%) doped CuO samples.

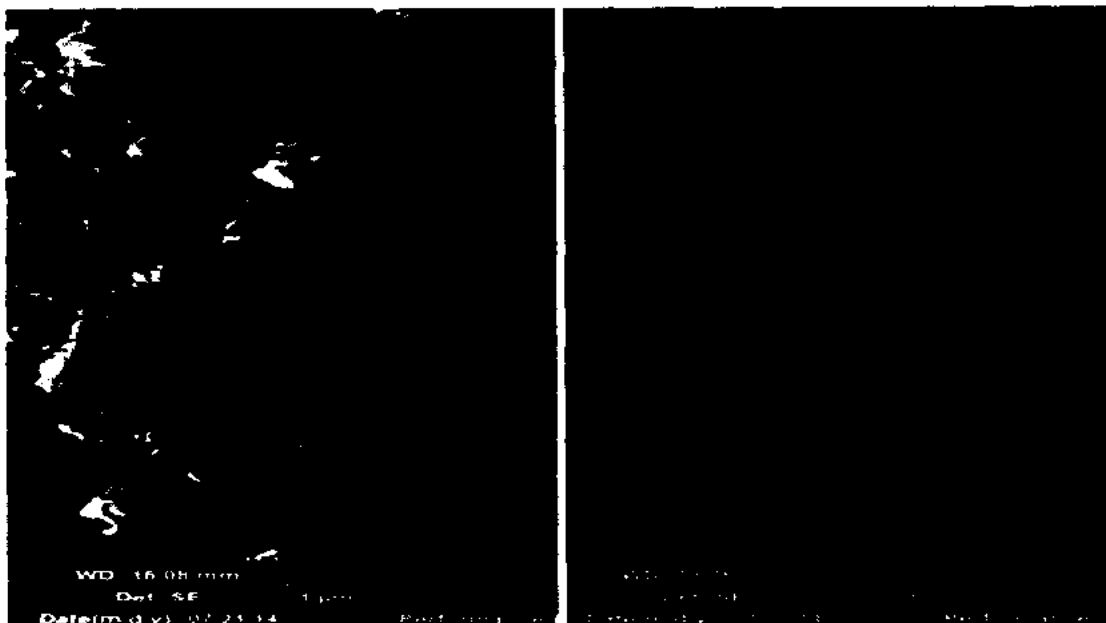


Figure 4.2 SEM images of undoped CuO samples

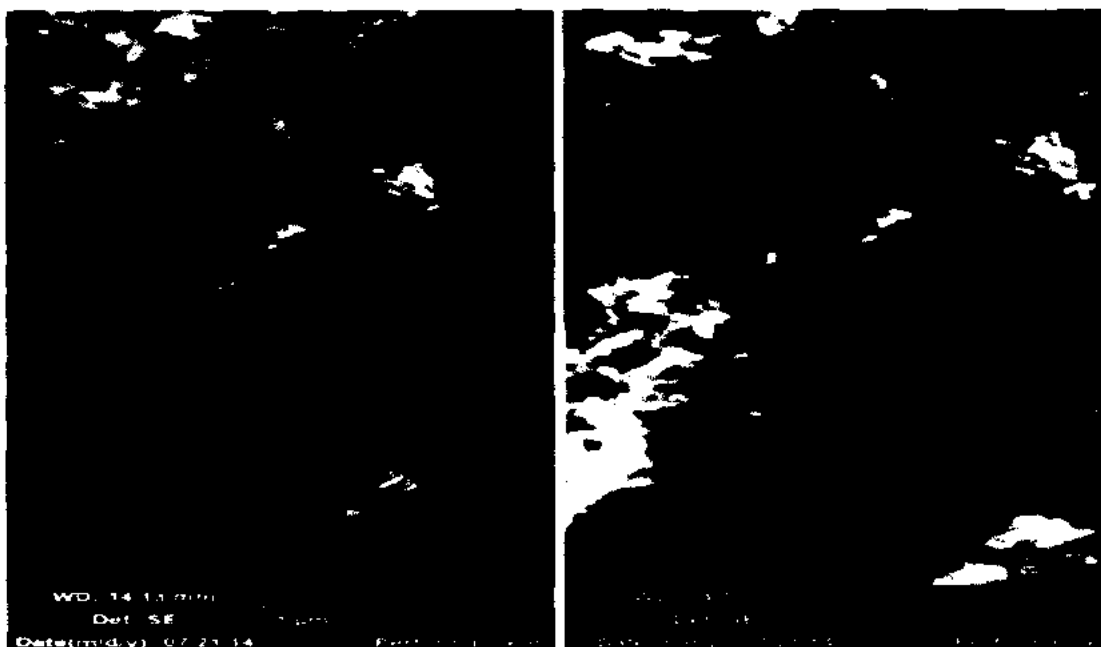


Figure 4.3 SEM images of 1% Fe doped CuO samples

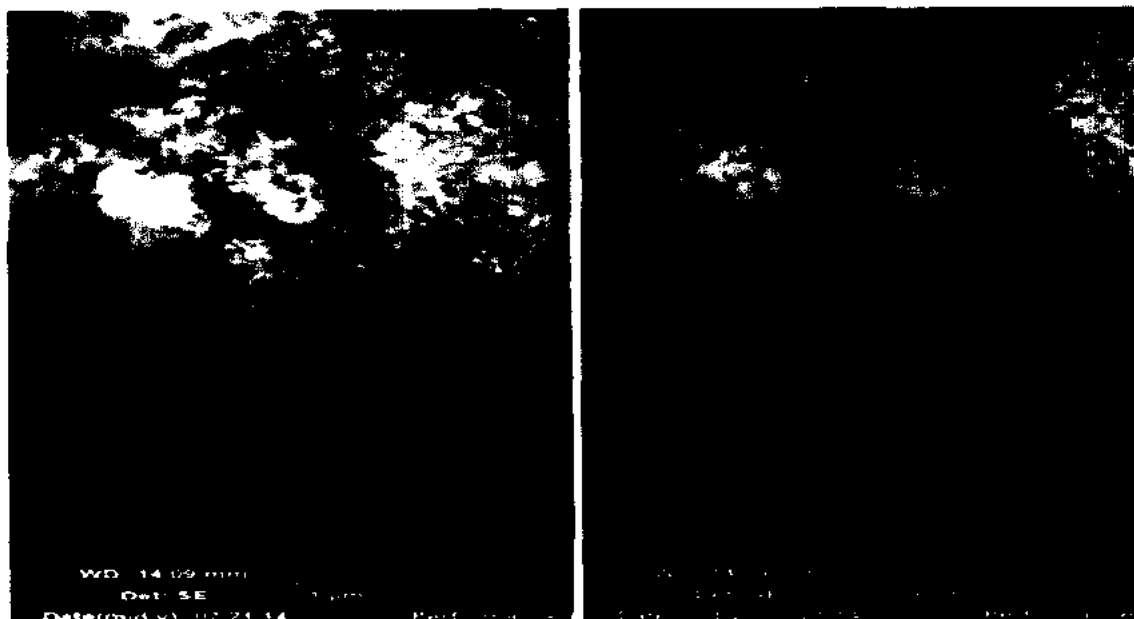


Figure 4.4 SEM images 5% Fe doped CuO sample

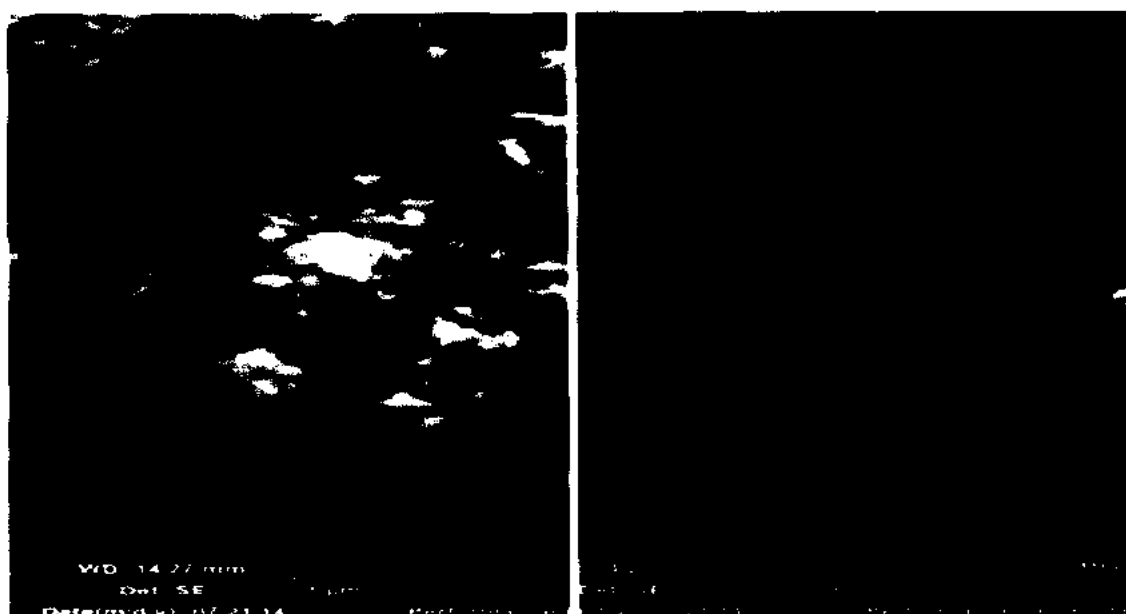


Figure 4.5 SEM images 7% Fe doped CuO sample

These figures show that nanostructures are formed. Fig 4.2 is of undoped CuO sample and is indicating that nanoparticles are formed and for Fe doping, the d size of particles is varying as shown in figs (4.2-4.5). This decrease is observed due to difference between the dopant and host matrix. In our case the host Cu^{2+} (0.73 Å) and dopant Fe^{3+} (0.64 Å) or Fe^{2+}

(0.74 Å) differ in radii as a result there is variation in size of particles from the pure sample [85].

4.3 Chemical Analysis

Energy dispersive x-ray spectroscopy results are considered to analyze the present composition of the materials and in each spectrum every element has its own characteristic peaks showing the presence in the tested samples. The EDS spectra results as well as percentage compositions are given in figures 4.6-4.10.

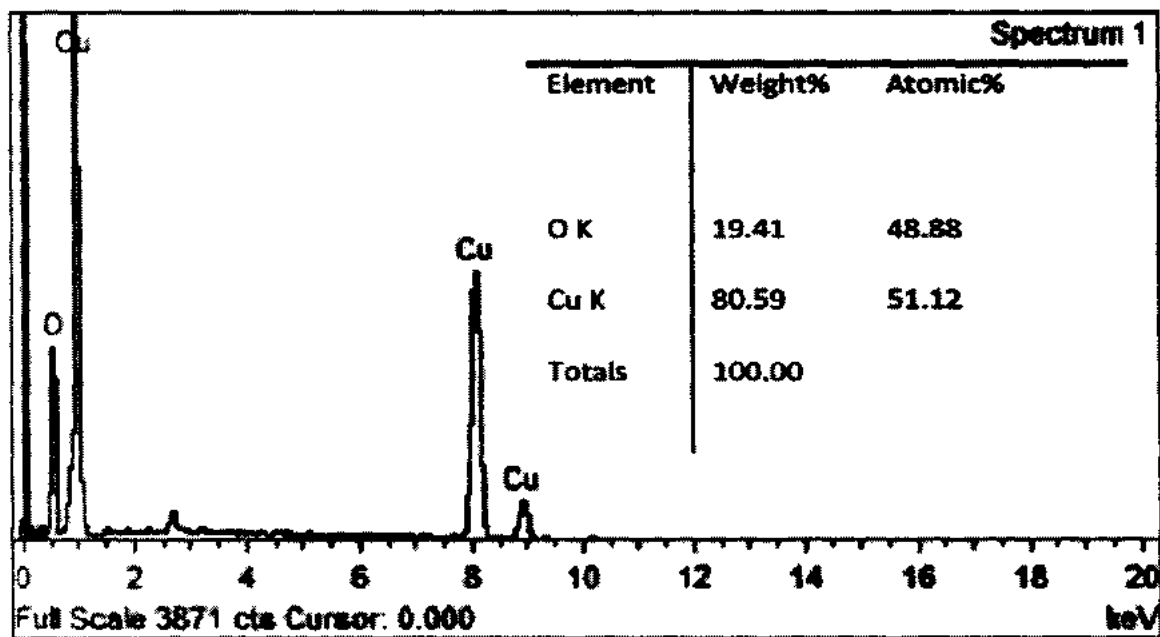


Figure 4.6 EDS spectrum of undoped CuO nanostructures

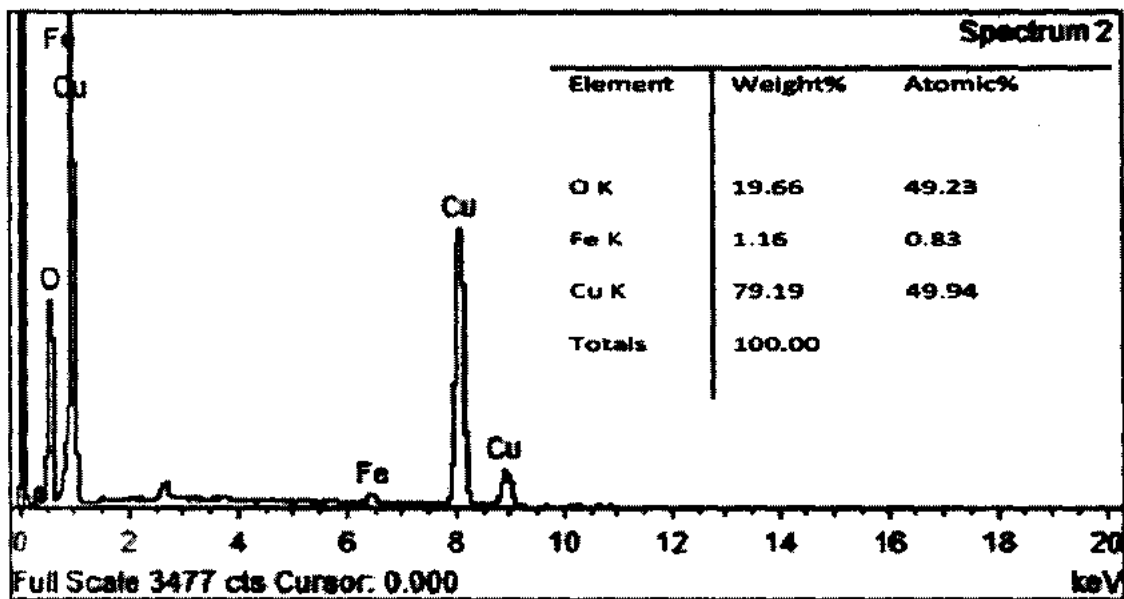


Figure 4.7 EDS spectrum of 1% Fe doped CuO nanostructures

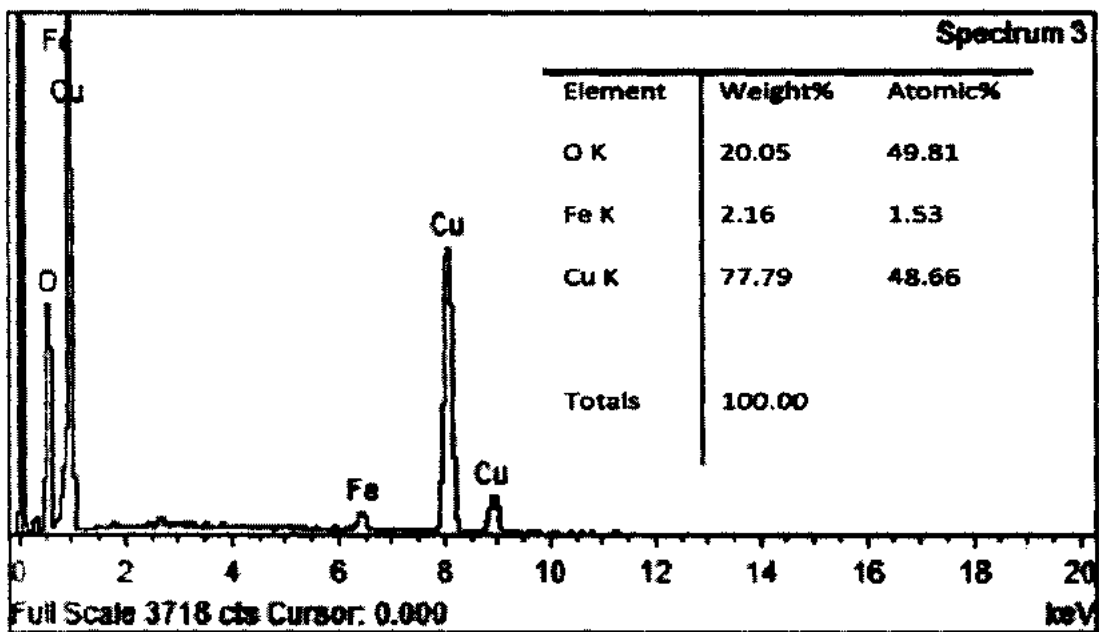


Figure 4.8 EDS spectrum of 3% Fe doped CuO nanostructures

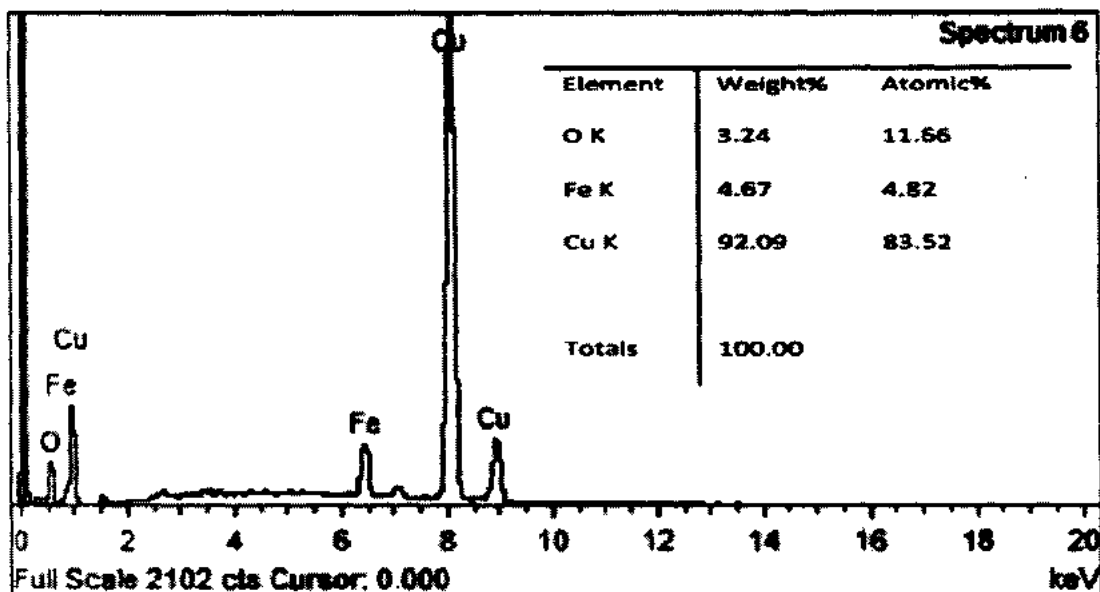


Figure 4.9 EDS spectrum of 5% Fe doped CuO nanostructures

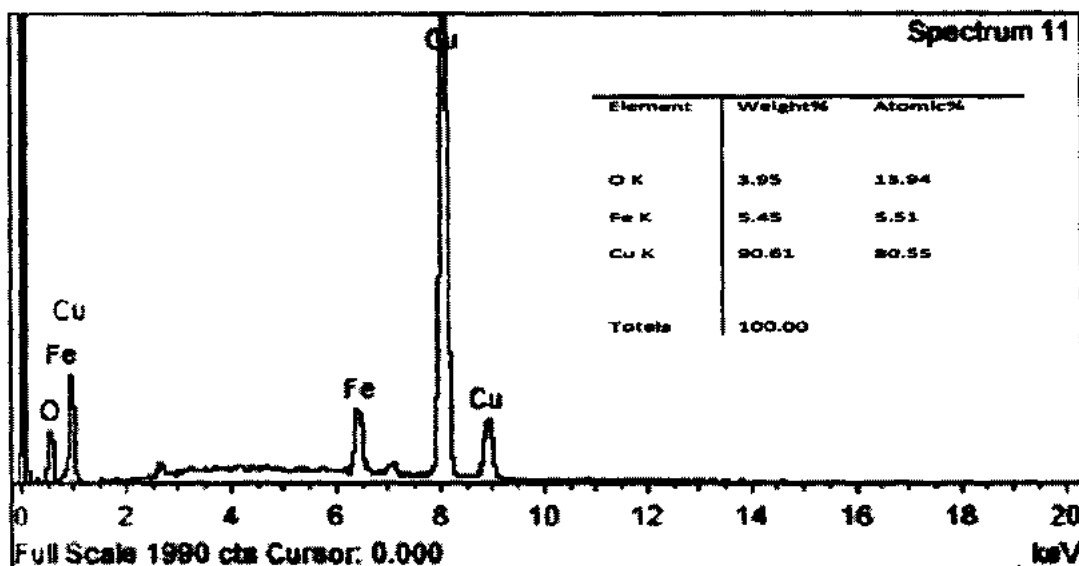


Figure 4.10 EDS spectrum of 7% Fe doped CuO

Fig 4.7 shows the undoped CuO in which only Copper (Cu) and Oxygen (O) are detected. While in fig 4.7-4.10 the elements in the products are Copper (Cu), Iron (Fe) and Oxygen (O) by a specific percentage showing the successful doping. Although the results are not exactly same as claimed but they favor the presence of copper, oxygen and iron which is

the proof that no extra element is included in materials which is supporting the XRD results of the obtained nanostructures.

4.4 Fourier Transform Infrared Spectroscopy (FTIR)

FTIR plots reveal the surface chemistry and modes of vibrations of chemical bond present in all the samples. Different FTIR spectra have been taken in the range of wavenumber 400 cm^{-1} to 4000 cm^{-1} for undoped CuO and 1% Fe doped CuO, 3% Fe doped CuO, 5% Fe doped CuO, and 7% Fe doped CuO and their spectral graphs are shown in Fig 4.11.

In the Fig 4.11 427 cm^{-1} , 511 cm^{-1} , 605 cm^{-1} , 1559 cm^{-1} , 2335 cm^{-1} and 3318 cm^{-1} are the main peaks observed at points a, b, c, d, e, f. In low frequency region three characteristic peaks shown in fig (a, b and c) are observed which are belong to the monoclinic structures of CuO [86]. No extra phase is observed of Fe or composite of CuFe. The peaks (d and f) belong to existence of water molecules which are may be adsorbed during the characterizing of samples. A weak peak is also observed at positioned (e) may due to CO_2 vibrations. The energies are shifted to higher values after doping of Iron.

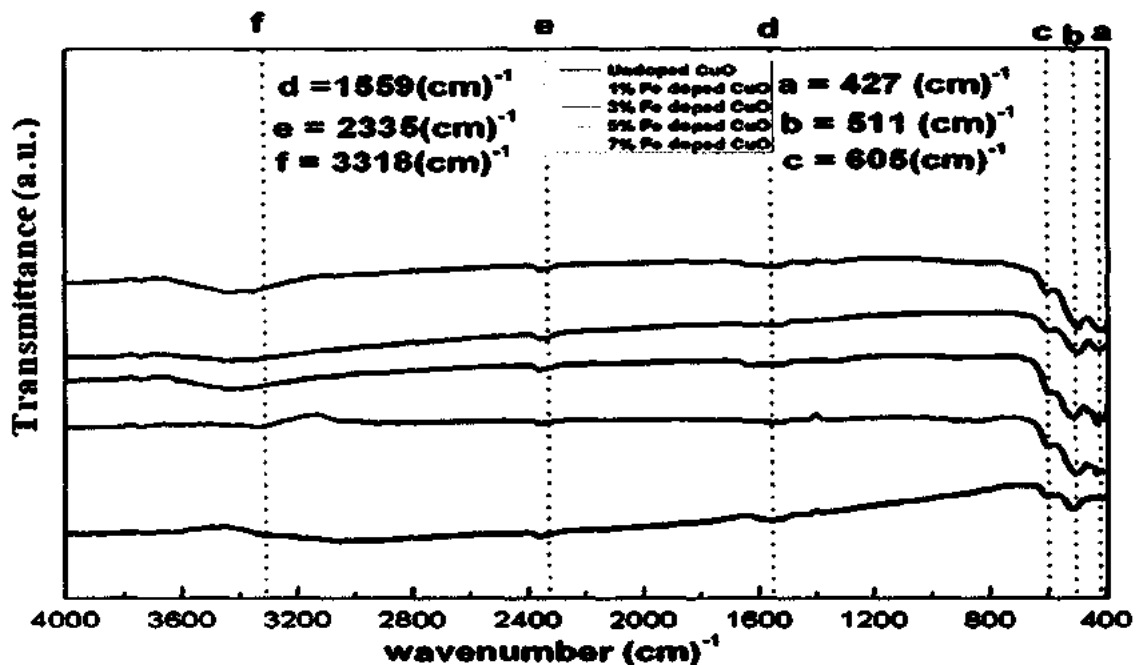


Figure 4.11 FTIR combined spectra for both doped and undoped CuO nanostructures

The FTIR study clearly confirms the successful doping of Fe doped CuO and formation of single monoclinic phase.

4.5 Optical Properties

The UV Vis DRS spectra have been used to study the optical band gap of undoped and Fe doped CuO nanostructures. The spectra have been recorded at the room temperature in the range of 200 nm and 800 nm wavelength.

The Kubelka munk function is used to find the values of band gap (BG)

$$f(R) = (1-R)^2/2R.....(4.2)$$

Where $f(R)$ is Kubelka Munk Function

R is reflectance

1-R is the absorbance of samples.

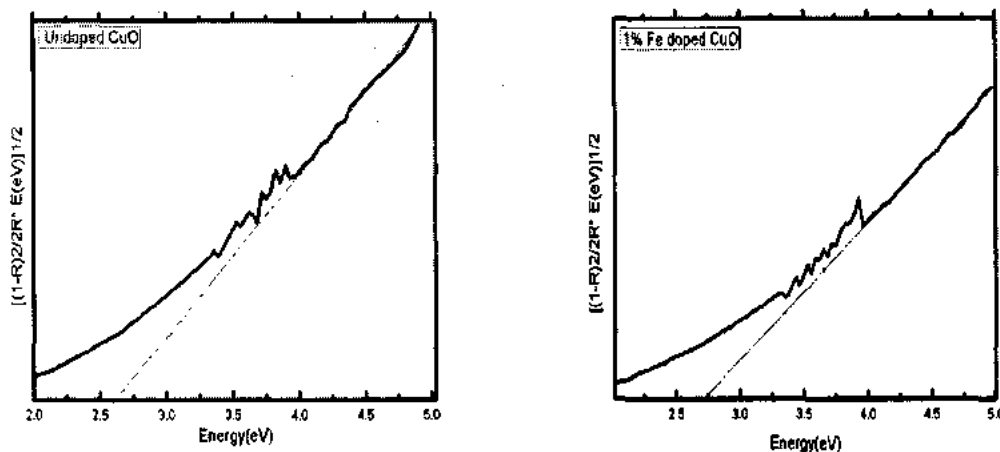


Figure 4.12 (a, b) DRS spectra of undoped CuO d 1% Fe doped CuO nanostructures

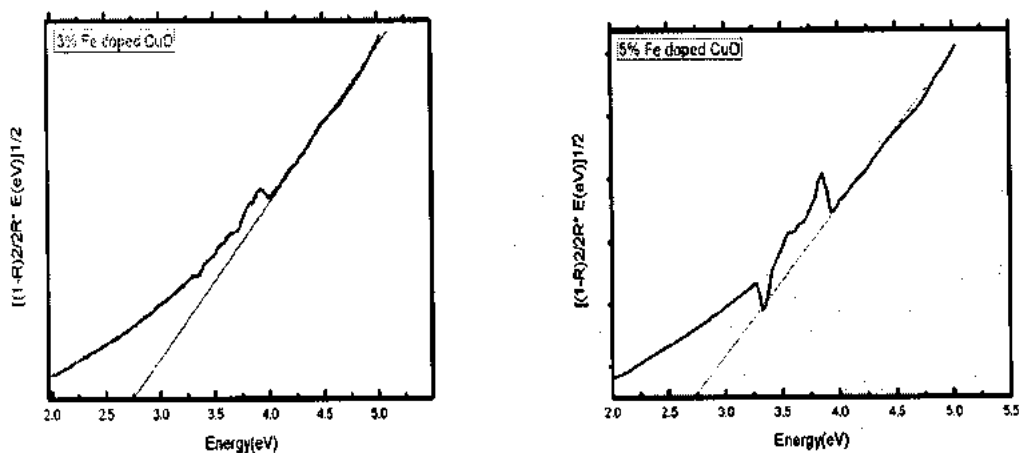


Figure 4.13 (a, b) DRS spectra of 3% and 5% Fe doped CuO nanostructures

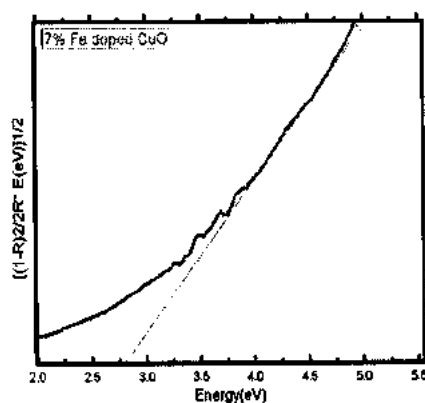


Figure 4.14 DRS spectra of 7% Fe doped CuO nanostructures

It has been interesting found that band gap measured from UV vis DRS spectra has significant shift from bulk CuO (1.2 eV) toward 2.1 eV [87]. The DRS visible spectroscopy absorption spectra have been plotted between energy ($h\nu$) and direct band gap $[(1-R)^2/2R * h\nu(eV)]^{1/2}$ are shown in figures 4.12(a, b), 4.13(a, b) and 4.14.

The estimated values of band gap are given in table 4.2. It has been significantly found that Fe doping has tuned the optical band gap of CuO. There is a red shift in the band gap as a function of Fe dopant concentration and all the results lie in agreement with the literature range 2.8 eV to 4.13eV [88-89].

Table 4.2 Estimated band gap for undoped and Fe doped CuO samples

Sample	Direct Band Gap (eV)
Undoped CuO	2.63
Fe _{0.01} Cu _{0.99} O	2.74
Fe _{0.03} Cu _{0.97} O	2.76
Fe _{0.05} Cu _{0.95} O	2.78
Fe _{0.07} Cu _{0.93} O	2.81

This red shift in band gap is consistent with particle size. As it is noted that with Fe doping the particle size is reduced as a result of quantum confinement the band gap is increased. This significant tailoring in direct band gap makes these nanostructures potential for optical nanodevices.

Conclusions

All study validates the successful synthesis of CuO and 1.0wt%, 3.0 wt%, 5.0 wt% and 7.0 wt% Fe doped nanostructures via simple hydrothermal method. The structural study through XRD indicates all peaks of monoclinic structure without interference of dopants which is positive conclusion about the formation of CuO nanostructures. By SEM, crystallite size is observed to decrease gradually with dopant concentration initially and finally increases. Energy dispersive Spectroscopy (EDS) have been performed to study the composition of elements present and as a result Cu and O are detected for undoped CuO while Cu, O and Fe are detected for Fe doped samples. For surface chemistry and vibrational modes Fourier transform infrared spectroscopy (FTIR) have been carried out. The stretched mode of Cu-O was shifted to higher energies because of dopant concentration and irregular change in grain size. For calculation of optical band gap, the diffuse reflectance UV visible spectroscopy have been done and band gap was found to be in the 2.63 eV for undoped CuO and 2.74-2.81 eV for Fe doped nanostructures. The successful doping of Fe into host matrix with nanostructures morphology and tunned bandgap make these prepared materials useful in different applications such as optical devices, solar cell technology and spintronics devices.

References

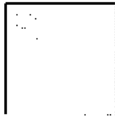
- [1] F Zhao, H M Qiu, L Q Pan, H Zhu, Y P Zhang, Z G Guo, John Q Xiao *J. Phys: Condense Matter* 20, 425208 (2008)
- [2] A Gennadiy, Takyuki *Japanes J. phy.* 39, 941-951 (2000)
- [3] Grundmann, Marius: *the Physics of Semiconductor* 2nd ed. (2010)
- [4] Zlatko MICKOVIĆ: *the Case of Transition Metal Doped ZnO Thesis* (2010)
- [5] M K Jain, *Diluted Magnetic Semiconductors* By world scientific publishers (1991)
- [6-] M Linnarsson, E Janzen, B Monemar, M Kleverman *Phys. Rev. B* 55, 6938 (1997)
- [7] C Timm *J. Phys. Condense. Matter* 15, 1865–1896 (2003)
- [8] S A Wolf, D D Awschalom, R A Buhrman *Material Sci.* 294, 1488-1495 (2001)
- [9] Awschalon, D D Flatte, M E *Nat. Phys.* 2, 153 (2007)
- [10] I Zutic, Jaroslav Fabian, S Das Sarma *Rev. Mod. Phys.* 76, 323 (2004)
- [11] T Dietl, J K Furdyna, *Science* 287, 1019 (2000)
- [12] C H Bennett, Di Vincenzo D P *Nature* 404, 247 (2000)
- [13] D Chiba, M Yamanouchi, F Matsu Kura, and H Ohno, *Science* 301,943 (2003)
- [14] A K Singh, T C Goel, R G Mendiratta, *J. Appl. Phys.* 91, 26-66 (2002)
- [15] Y W Heo, M P Iivil, K Ip *Appl. Phys. Lett.* 84, 2292 (2004)
- [16] SW Jung, S J An, H Kim, D Kim *Appl. Phys. Lett.* 80, 4561 (2002)
- [17] N Theodoropoulou A F Hebard *Phys. Rev. Lett.* 89, 107203 (2002)
- [18] M L Reed , N El-Masry, H H Stadelmaier, M K Ritums, *Appl. Phys. Lett.* 79, 3473 (2001)
- [19] X Chen, HQ Song, YX Chen, MJ Ren, *Appl. Phys. Lett.* 81, 51 (2002)
- [20] Y D Park Ambrose, A Wilson, G Spanos, B T Jonker *Science* 295, 652 (2002)
- [21] A Osterloh, L Amico, G Fazio, *Nature* 416, 608-610 (2002)
- [22] F Zhao, H M Qiu, L Q Pan, H Zhu, Y P *Phys. Condense. Matter* 20, 425208–425215 (2008)
- [23] A Filip petti, V Fiorentini, *Phys. Rev. B* 74, 220401-4 (2006)
- [24] S G Yang T Li, B X Gu, Y W Du *Appl. Phys. Lett.* 83, 3746–3753 (2003)

- [25] M Tseggai, R Tellgren, P Nordblab Sci. Technol. 61, 1651-1662 (2005)
- [26] K W Wagner Ann. Phys. 40,817 (1913)
- [27] C F Jafferson, C K Baker IEEE Trans. Magn. App. phy. 34, 44-60 (1968)
- [28] Buzea, Cristina, Pacheco et al: Sources and Toxicity". Bio inter phases 2, 17-71(2007)
- [29] P S Kumar, S. Kumar, R. C. Savadi, Jins John, J. Indian Prosthodont Soc.,11(1), 1-6 (2011)
- [30] G Vastola .Current Opinion in Solid State & Materials Science, 16(2), 64 (2012)
- [31] Ou Chen, Nature Materials 10, 3539 (2013)
- [32] Z Gao , X Liang, T Pereira, R Scaffaro, H HahnComposites Science and Technology 67, 2036–2044 (2007)
- [33] J N Tiwari, R N Tiwari, K S Kim. Prog Mater Sci; 57,724–803(2012)
- [34] P Lignier, R Bellabarba, RPR Tooze. Chem Soc. Rev.41, 1708–20 (2012)
- [35] X, Chen S Mao Chem Rev; 107, 2891–959(2007)
- [36] J Park, J Joo, SG Kwon ,Y Jang ,T Hyeon Angew Chem. Int. Ed. 46,4630–60 (2007)
- [37] H Zheng ,J Zhen Ou , S Michael, Strano Adv. Funct. Mater. 21, 2175–96(2011)
- [38] D P Singh, N Ali, J. Sci. Adv. Mater. 2,295–335 (2010)
- [39] S Anandan, S Yang J. Exp. Nanosci.2, 23–56 (2007)
- [40] A N Banerjee et.al J. Progr in Crystal Growth and Characterization of Material 52-105 (2005)
- [41] Kodeh Fawzi e.al J. NanoLett. 2, 14 (2012)
- [42] B Meyer et al. Phy.Status Solidi.249,1487–509 (2012)
- [43] S Asbrink, L J Norr by Found Crystallogr. 26, 8(1970)
- [44] M K Song, S Park, FM Alamgir, J Cho, M Liu J .Mater Sci Eng R Rep.72, 203–52 (2011)
- [45] V V Kislyuk, OP Dimitriev. J Nanosci Nanotechnology; 8,131–48 (2008)
- [46] S BB Wang, CHH Hsiao, SJJ Chang, Lam. KTT, Wen Sensor Actuat.A Phys.171, 207–11 (2011)
- [47] C Rossi, K Zhang, G Rodrigue J. Micro electromech Syst. 16,919–31 (2007)
- [48] L P Zhou, B X Wang, X F Peng, X Z Du, Y P Yang Adv. Mech. Eng. 20,1–4 (2010)
- [49] M M Rahman, J Saleh Ahammad, J H Jin Sensors 10, 4855–86(2010)
- [50] KJ Choi, H W Jang Review and Issues Sensors 10, 4083–99 (2010)

- [51] I Ali New generation adsorbents for water treatment *Chem. Rev.* 112, 5073–91 (2012)
- [52] Yu X-Y *ACS Appl. Mater Interfaces* 4, 1954–62 (2012)
- [53] X Zhang et al. *ACS Nano*. 5, 2013–19 (2011)
- [54] J Liu *J. Colloid Interface Sci.* 384, 1–9 (2012)
- [55] YW Zhu , T Yu, F C Cheong, X J Xu, C T Lim, V B C Tan, *J. Nanotechnology* 16,88–92 (2005)
- [56] R Kumar ,Y Diamant ,A Gedanken *J. of Chem Mater.* 12:2301–5(2000)
- [57] X Li , C Wang *J. Mater. Chem. A* 1, 165–82 (2013)
- [58] S Venkatachalam, H Zhu, C Masarapu, K Hung, Z Liu *ACS Nan.*3,2177–84 (2009)
- [59] P Poizot, S Laruelle, S Grugeon, L Dupont, J M Tarascon *J. of. Nature* 407,496–9 (2000)
- [60] S F Zheng, J S Hu, L S Zhong, W-G Song, L-J Wan *J. Alloys Compd.* 20,3617–22(2008)
- [61] X Guan, L Li , G Li ,Z Fu , J Zheng , T Yan *J. Alloys Compd.* 509, 3367–74 (2011)
- [62] S Gao , S Yang ,J Shu ,S Zhang ,Z Li ,K Jiang *J. Phys. Chem.C*112, 19324–28 (2008)
- [63] J Gao et al.. *J. Phy. Chem. B* 108, 5547–51 (2004)
- [64] X Zhang , D Zhang , X Ni , J Song , H Zheng . *J. Nanopart. Res.* 10,839–44 (2007)
- [65] J H Ju. K-S Ryu. *J. Electrochem. Soc.* 158, 814 (2011)
- [66] Amin G 1st ed. LiU-Tryck: Norrköping (Sweden) SE-60174(2012)
- [67] B Meyer , A Polity , D Reppin , M Becker , et al *Phys Status Solidi.*249,1487–509 (2012)
- [68] X Chen, S Mao *Chem. Rev.* 107,2891–959 (2007)
- [69] J Park , J Joo , SG Kwon,Y Jang ,T Hyeon *Angew. Chem. Int Ed.* 46,4630–60 (2007)
- [70] R Devan , R Patil ,J Lin ,Y Ma *Adv. Funct. Mater.* 22, 3326–70 (2012)
- [71] C Jagadish, S J. Perrton Elsevier, New York 2nd Edition (2006)
- [72] J V Stark, K. J Klabunde, *J. Chem. Mater.* 8, 1913 (1996)
- [73] K Maaz et.al *Journal of Magnets and Magnetic Materials*, 321, 1838-1842(2009)
- [74] Z Zhuang, Q Peng ,Y Li .*Chem. Soc. Rev.* 40,5492–513(2011)
- [75] K Byrappa, Masahiro Yoshimura *A hand book on hydrothermal Technology* (2012)
- [76] B D Cullity, A Wesley London, *elements of X-ray diffraction* 10, 73-80 (1959)
- [77] David Williams , Barry Carter *Tb material science* ISBN 978-0-387-76500-6 90 (2009)

- [78] B C Smith, *Fundamentals of Fourier Transform Infrared Spectroscopy*, CRC press (1996)
- [79] B H Charles, J M Wofford, E Starodub, A L Walter, S Nie, A. Bostwick, N C Bartelt *J. Appl. Phys.* 111, 321 (2012)
- [80] R Adhikari, A K Das, D Karmakar, T C Rao, *Physical Review B* 78, 024404 (2008)
- [81] L M Fang, X T Zu, Z J L *Journal of Alloys and Compounds* 454, 261 (2008)
- [82] A Gordon *Physics Faculty Publications and Presentations* 4-1(2012)
- [83] NM Basith, JJ Vijaya, LJ Kennedy, M Bououdina *Physica E* 53, 193–199 (2013)
- [84] KK Dey, JS Tawale, KK Dey, R Pasricha, KN Sood, AK Srivastava ... R Shanker, A Dhawan, M Wan, RR Yadav. *RSC Adv.*2, 1387 (2012)
- [85] N Sharma, S Sharda, Vineet Sharma, Pankaj Sharma *Journal of Magnetism and Magnetic Materials* 377,183–189 (2015)
- [86] L Saviot, D Machon, L Debbichi, A Girard, J Margueritat, P Krueger, M. C. Marco de Lucas *J. Phys. Chem. C* 116 10232–10237 (2012)
- [87] A Azam, A Jawad, AS Ahmed. *J. Alloys and Compounds* 509, 2909(2011)
- [88] A Ogwu, T Darma, E Bouquerel *J. Achiev Mater Manufact. Eng.* 24,172–7(2007)
- [89] K Borgohain, S Mahamuni. *J. Mater. Res.*17, 1220–3(2002)

Plagiarism Report



Turnitin Originality Report

2015 Thesis: Study of Fe Doped Induced Effects on Physical Properties of CuO Nanostructures by Asghar Ali

From BS, MS and PhD Thesis (BS, MS, Ph.D Thesis Plagiarism)

Dr. Javed Iqbal Saggu
 Assistant Professor (Physics)
 International Islamic University
 Islamabad.

Similarity Index 10%	Similarity by Source	
	Internet Sources:	2%
	Publications:	6%
	Student Papers:	4%

Processed on 03-Jul-2015 11:15 PKT
 ID: 553860992

sources:

Word Count: 7994

- 1** 2% match (publications)

Zhang, Qiaobao, Kaili Zhang, Daguo Xu, Guangcheng Yang, Hui Huang, Fude Nie, Chenmin Liu, and Shihe Yang. "CuO nanostructures: Synthesis, characterization, growth mechanisms, fundamental properties, and applications". Progress in Materials Science, 2014.
- 2** 1% match (publications)

Byrappa, K., and Masahiro Yoshimura. "History of Hydrothermal Technology". Handbook of Hydrothermal Technology, 2013.
- 3** 1% match (publications)

Mohamed Basith, N., J. Judith Vijaya, L. John Kennedy, and M. Bououdina. "Structural, optical and room-temperature ferromagnetic properties of Fe-doped CuO nanostructures". Physica E Low-dimensional Systems and Nanostructures, 2013.
- 4** < 1% match (student papers from 30-May-2012)

Class: Quick Submit
 Assignment:
 Paper ID: 252322368
- 5** < 1% match (student papers from 03-Dec-2008)

Submitted to Temple University on 2008-12-03
- 6** < 1% match (student papers from 18-Dec-2014)

Submitted to Higher Education Commission Pakistan on 2014-12-18
- 7** < 1% match (publications)

William Martin. "Atomic Spectroscopy", Springer Handbook of Atomic Molecular and Optical Physics, 2006
- 8** < 1% match (Internet from 17-Apr-2015)

...

- 9 < 1% match (publications)
Carsten Timm, "Disorder effects in diluted magnetic semiconductors", Journal of Physics Condensed Matter, 12/24/2003
-
- 10 < 1% match (student papers from 09-Dec-2009)
Submitted to Higher Education Commission Pakistan on 2009-12-09
-
- 11 < 1% match (publications)
D. K. Avasthi, "Materials Engineering with Swift Heavy Ions", Springer Series in Materials Science, 2011
-
- 12 < 1% match (student papers from 25-May-2011)
Submitted to BITS, Pilani-Dubai on 2011-05-25
-
- 13 < 1% match (student papers from 04-Jun-2015)
Submitted to Universiti Malaysia Perlis on 2015-06-04
-
- 14 < 1% match (Internet from 19-Jan-2015)
http://thermec.org/template3s/Abstract_book_Final.pdf
-
- 15 < 1% match (publications)
AOUAK, TAIEB; DERAZ, NASRALLAH and ALARIFI, ABDULLAH, "Synthesis, non-isothermal crystallization and magnetic properties of CoZnFeO/poly(ethylene-co-vinyl alcohol) nanocomposite", Bulletin of Materials Science, 2013.
-
- 16 < 1% match (Internet from 15-Jan-2013)
[http://en.wikipedia.org/wiki/Copper_\(II\)_oxide](http://en.wikipedia.org/wiki/Copper_(II)_oxide)
-
- 17 < 1% match (publications)
Jan, Tariq, Javed Iqbal, Qaisar Mansoor, M Ismail, M Sajjad Haider Naqvi, Asma Gul, S Faizan-ul-Hassan Naqvi, and Fazal Abbas, "Synthesis, physical properties and antibacterial activity of Ce doped CuO: a novel nanomaterial", Journal of Physics D Applied Physics, 2014.
-
- 18 < 1% match (student papers from 10-Dec-2009)
Submitted to Higher Education Commission Pakistan on 2009-12-10
-
- 19 < 1% match (student papers from 16-Jan-2014)
Submitted to Higher Education Commission Pakistan on 2014-01-16
-
- 20 < 1% match (Internet from 19-May-2015)

http://archive.org/stream/ChemicalProcessDynamicsAndControls/ChemicalProcessDynamicsAndControls_djvu.txt

- 21 < 1% match (student papers from 12-May-2014)
Submitted to Malaviya National Institute of Technology on 2014-05-12
- 22 < 1% match (Internet from 29-Apr-2014)
<http://www.azonano.com/article.aspx?ArticleID=3782>
- 23 < 1% match (publications)
Sangchay Weerachai, Mudtharak Weerachai, Mahamad Kuntapon and Namesai Aurasu, "The Physical Properties and Photocatalytic Activity of Cu/TEA Doped TiO₂-Nanoparticles Prepared by the Sol-Gel Process", Journal of Chemistry & Chemical Engineering, 2012.
- 24 < 1% match (student papers from 08-May-2010)
Submitted to October University for Modern Sciences and Arts (MSA) on 2010-05-08
- 25 < 1% match (student papers from 04-Aug-2010)
Submitted to Universiti Putra Malaysia on 2010-08-04
- 26 < 1% match (student papers from 23-Feb-2015)
Submitted to Higher Education Commission Pakistan on 2015-02-23
- 27 < 1% match (publications)
Tinh, Than Xuan, Nguyen Van Chuc, Vincent Jourdain, Matthieu Paillet, Do-Yoon Kim, Jean-Louis Sauvaiol, Ngo Thi Thanh Tam, and Phan Ngoc Minh, "Synthesis of individual ultra-long carbon nanotubes and transfer to other substrates", Journal of Experimental Nanoscience, 2011.
- 28 < 1% match (student papers from 04-Aug-2010)
Submitted to Atlantic International University on 2010-08-04
- 29 < 1% match (Internet from 29-Mar-2015)
- 30 < 1% match (Internet from 19-Oct-2009)
<http://archiv.tu-chemnitz.de/pub/2008/0135/data/Thesis.pdf>
- 31 < 1% match (publications)
Moody, "Laboratory Analyses", Nuclear Forensic Analysis, 2005.

< 1% match (Internet from 08-Feb-2010)

- 32 <http://electroceramica.ciceco.ua.pt/Abstract%20book.pdf>
- 33 < 1% match (Internet from 25-Jan-2014)
<http://www.china-sourcing.org/index.php/easyblog/plastic-flexible-packaging-material.html>
- 34 < 1% match (publications)
[Hongshi Zhao. "Biomimetic Synthesis and Characterization of Hydroxyapatite Crystal with Low Phase Transformation Temperature", Journal of Chemical & Engineering Data, 12/11/2008](#)
- 35 < 1% match (publications)
[David A. Litton. "Molecular Dynamics Simulations of Calcium Aluminosilicate Intergranular Films on \(0001\) Al₂O₃ Facets", Journal of the American Ceramic Society, 12/20/2004](#)
- 36 < 1% match (Internet from 01-Mar-2015)
<http://www.science.gov/topicpages/m/macroporous+polyglycidyl+methacrylate-co-ethylene.html>
- 37 < 1% match (Internet from 13-Sep-2014)
<http://www.science.gov/topicpages/z/zinc+oxide+izo.html>
- 38 < 1% match (publications)
[Basith, N. Mohamed, J. Judith Vijaya, and L. John Kennedy. "Structural, Morphological, Optical, and Magnetic Properties of Fe-Doped CuO Nanostructures", Advanced Materials Research, 2014.](#)
- 39 < 1% match (publications)
[Nehru, L.C., V. Swaminathan, M. Jayachandran, and C. Sanjeeviraja. "Nanomaterial Preparations by Microwave-Assisted Solution Combustion Method and Material Properties of SnO₂ Powder - A Status Review", Materials Science Forum, 2011.](#)
- 40 < 1% match (publications)
[OSIKOYA, A. O.; WANKASI, D.; VALA, R. M. K.; DIKIO, C. W.; AFOLABI, A. O.; AYAWEI, N. and DIKIO, E. D. "SYNTHESIS, CHARACTERIZATION AND SORPTION STUDIES OF NITROGEN-DOPED CARBON NANOTUBES", Digest Journal of Nanomaterials & Biostructures \(DJNB\), 2015.](#)
- 41 < 1% match (student papers from 14-Jan-2015)
[Submitted to Higher Education Commission Pakistan on 2015-01-14](#)

paper text:

Asghar Ali Abstract Metal oxides specially diluted magnetic oxides have unique size and dimensionally dependent chemical and physical properties and therefore have achieved too much attraction of